The Meteoritical Society

Meteoritics & Planetary Science 44, Nr 5, 701–724 (2009)
Abstract available online at http://meteoritics.org

On the origin of shocked and unshocked CM clasts in H-chondrite regolith breccias

Alan E. RUBIN[1] and William F. BOTTKE[2]

[1]Institute of Geophysics and Planetary Physics, University of California, Los Angeles, California 90095–1567, USA
[2]Southwest Research Institute, 1050 Walnut St., Suite 400, Boulder, Colorado 80302, USA
*Corresponding author. E-mail: aerubin@ucla.edu

(Submitted 26 September 2008; revision accepted 19 February 2009)

Abstract—CM chondrite clasts that have experienced different degrees of aqueous alteration occur in H-chondrite and HED meteorite breccias. Many clasts are fragments of essentially unshocked CM projectiles that accreted at low relative velocities to the regoliths of these parent bodies. A few clasts were heated and dehydrated upon impact; these objects most likely accreted at higher relative velocities. We examined three clasts and explored alternative scenarios for their formation. In the first scenario, we assumed that the H and HED parent bodies had diameters of a few hundred kilometers, so that their high escape velocities would effectively prevent soft landings of small CM projectiles. This would imply that weakly shocked CM clasts formed on asteroidal fragments (family members) associated with the H and HED parent bodies. In the second scenario, we assumed that weakly shocked CM clasts were spall products ejected at low velocities from larger CM projectiles when they slammed into the H and HED parent bodies. In both cases, if most CM clasts turn out to have ancient ages (e.g., ~3.4–4.1 Ga), a plausible source for their progenitors would be outer main belt objects, some which may have been dynamically implanted 3.9 Ga ago by the events described in the so-called "Nice model." On the other hand, if most CM clasts have recent ages (<200 Ma), a plausible source location for their parent body would be the inner main belt between 2.1–2.2 AU. In that case, the possible source of the CM-clasts' progenitors' parent fragments would be the breakup ~160 Ma ago of the parent body 170 km in diameter of the Baptistina asteroid family (BAF).

INTRODUCTION

CM-chondritic material is ubiquitous in the inner solar system. CM chondrites are the most abundant group among carbonaceous-chondrite falls and finds on Earth (Grady 2000). The majority of unmelted micrometeorites also appear to be CM chondrites (e.g., Kurat et al. 1994; Walter et al. 1995; Yada et al. 1997). One of the rare meteorites recovered from the Moon appears to have been derived from a CM projectile (McSween 1976; Zolensky et al. 1996). Approximately 1–2% of lunar maria soils consist of a meteorite component most similar to CM chondrites (Wasson et al. 1975).

CM-chondrite clasts are the most abundant variety of foreign materials in H-chondrite regolith breccias (e.g., Fodor and Keil 1976; Fodor et al. 1976; Keil and Fodor 1980; Nozette and Wilkening 1982; Lipschutz et al. 1989), constituting, by our estimation, ~1–3 vol% of Abbott (H). CM clasts are also the most abundant foreign materials in HED breccias (Wilkening 1973; Bunch et al. 1979; Kozul and Hewins 1988; Pun 1992; Zolensky et al. 1992; Buchanan et al. 1993; Brearley 1993; Zolensky et al. 1996; Gounelle et al. 2003), constituting ~5 vol% of the Kapoeta howardite (Zolensky et al. 1996).

Many foreign clasts in chondrite breccias were significantly shocked or impact-melted when they accreted to their host parent bodies. For example, an LL5 clast in the Dimmitt H-chondrite regolith breccia is significantly shocked and contains melt pockets produced in situ, presumably during accretion of the clast's projectile progenitor to the H-chondrite regolith (Rubin et al. 1983). An EH clast in the Galim LL6 polymict breccia has been shocked and oxidized (Christophe Michel-Lévy and Bourot-Denise 1988; Rubin 1997a). An igneous-textured clast with H-chondrite-like bulk and mineral compositions within the Ngawi LL regolith breccia is probably an impact-melted H-chondrite projectile (Fodor and Keil 1975). Another igneous clast with H-chondrite-like bulk-chemical, mineralogical and O-isotopic compositions in the Bovedy L-chondrite breccia (Rubin et al. 1981) probably has a similar origin. It is therefore remarkable

that many of the CM clasts in H-chondrite and HED breccias appear to be hydrated and relatively unshocked.

To address the origin of these unusual hydrated clasts, we studied three CM clasts in two solar-gas-rich H-chondrite regolith breccias: AB3 and AB8 from Abbott and PV3 from Plainview (1917), hereafter Plainview. The latter clast was initially described by Fodor and Keil (1976). Our analysis is given below.

The presence of weakly shocked hydrated objects in some regolith breccias may be used to gain insight into the evolution of the H-chondrite and HED parent bodies as well as that of the ultimate source of the CM clasts. This is a challenging task, in part because we lack a full understanding of the evolution of the main asteroid belt but also because the true sources of the H chondrites and CM clasts have yet to be identified. Nevertheless, we believe it is useful to try to place these samples into the context of our current understanding of main-belt history and discuss the strengths and weaknesses of several plausible formation scenarios.

In our first formation scenario, we postulate that the CM clasts formed on ancient family members (i.e., collisional fragments) of the H-chondrite and HED meteorite families. We favor formation on family members rather than on original meteorite parent bodies because the escape velocity from objects 200–500 km in diameter (the likely range in diameters of the H and HED parent bodies) is so high that the impact velocity of the progenitors is likely to have caused the CM clasts to become shocked and dehydrated.

In our second formation scenario, we discuss whether the CM clasts were delivered by larger, high-velocity projectiles via spallation. In both scenarios, we speculate that the sources of the CM material were primitive bodies implanted in the outer main belt ~3.9 Ga as a byproduct of the so-called Nice model that modified the architecture of the solar system and most likely produced the lunar Late Heavy Bombardment (Gomes et al. 2005; Morbidelli et al. 2005; Tsiganis et al. 2005; Levison et al. 2009).

Finally, in our third formation scenario, we examine whether the recent breakup of the Baptistina asteroid family in the inner main belt (Bottke et al. 2007), which happened to occur near a likely meteoroid supply route, might have produced the hydrated CM clasts.

ANALTYICAL PROCEDURES

Clast AB3 is from Abbott section UNM 3, clast AB8 is from Abbott section UNM 8, and clast PV3 is from Plainview section UNM 511. The UNM sections are from the Institute of Meteoritics, University of New Mexico.

We prepared mosaics of moderately high-resolution (2 μm/pixel) back-scattered electron (BSE) images of the three clasts. A 100 μm grid was superimposed on each image. The images were made with the LEO 1430 VP scanning electron microscope (SEM) at UCLA using a 15 keV accelerating voltage and a working distance of ~26 mm. We also made 10-element X-ray maps of the clasts using the JEOL JXA-8200 electron microprobe at UCLA.

The bright, somewhat irregularly shaped, Fe-rich clumps observed in BSE images of clasts AB3 and AB8 are inferred to be intergrowths of tochilinite (an interstratified Fe-Ni sulfide and Fe-Mg hydroxide; 2[(Fe,Mg,Cu,Ni[ ])S]-1.57–1.85[(Mg,Fe,Ni,Al,Ca)$(OH)_2$], where the open bracket represents a vacancy) and cronstedtite (an Fe-bearing serpentine; $Fe_2^{+2}Fe^{+3}(Si,Fe^{+3})_2O_5(OH)_4$).

Modal abundances of sulfide, silicates, and oxides were determined microscopically at high magnification in reflected light using an automated point counter. Metallic Fe-Ni is rare in the clasts; its modal abundance was determined directly by measuring the surface area of each small grain and comparing it to the total area of each clast. The modal abundances of large clumps of tochilinite-cronstedtite were estimated from the BSE images; the approximate abundance of carbonate was estimated from the multi-element X-ray maps.

The compositions of minerals and clumps of tochilinite-cronstedtite were determined with the JEOL electron microprobe using natural and synthetic standards, an accelerating voltage of 15 keV, 20 s counting times per element, ZAF corrections and a focused beam. The sample current was 6 nA for tochilinite-cronstedtite and 15 nA for other analyzed phases. The tochilinite-cronstedtite intergrowths are too fine-grained to allow individual minerals to be analyzed; thus, the tochilinite-cronstedtite analyses represent bulk compositions. The "FeO" concentration includes FeO from phyllosilicates, Fe^{3+} in cronstedtite, and Fe^{2+} in sulfides. Following the procedures of Rubin et al. (2007), we deleted all analyses with totals outside the range 74–93 wt% and all analyses with <10 wt% SiO_2. About 28% of the tochilinite-cronstedtite analyses of clast AB3 were discarded on this basis; no tochilinite-cronstedtite analyses were discarded from clast AB8. Tochilinite-cronstedtite is absent from clast PV3.

The bulk composition of the PV3 rim was determined by averaging the composition of two representative 100 × 100 μm grids at different sides of the PV3 clast. There were 10 rows and 10 columns in each grid; a 6 μm wide electron beam was used. All Fe was calculated as FeO. No points were discarded from the 200 analyses.

RESULTS

Petrology of Abbott and Plainview

Abbott (Fodor et al. 1976) and Plainview (Fodor and Keil 1976) are solar-gas-rich (Schultz and Kruse 1989) H-chondrite regolith breccias possessing a light/dark structure consisting of light-colored, metamorphosed (type-4 to 6) H-chondrite clasts embedded in a dark-colored gas-rich clastic matrix. Also present are impact-melt-rock clasts, shock-

Table 1. Olivine and low-Ca pyroxene compositions (wt%) in the CM clasts.

	AB3	AB8	PV3 interior	PV3 rim	Plainview host
Olivine					
No. of points	26	7	24	39	47
SiO_2	41.9 ± 1.5	41.5 ± 2.0	42.4 ± 0.6	41.0 ± 1.5	39.4 ± 0.21
FeO	4.6 ± 8.0	5.9 ± 10.6	1.9 ± 2.6	10.1 ± 8.1	16.9 ± 0.6
Cr_2O_3	0.48 ± 0.25	0.33 ± 0.12	0.33 ± 0.14	0.25 ± 0.20	<0.04
MgO	53.3 ± 6.3	51.8 ± 8.4	54.8 ± 2.4	48.6 ± 6.4	43.9 ± 0.5
CaO	0.25 ± 0.10	0.26 ± 0.10	0.30 ± 0.28	0.24 ± 0.19	<0.04
total	100.5	99.8	99.7	100.2	100.2
Fa (mol%)	4.9 ± 8.9	6.5 ± 12.0	2.0 ± 2.7	10.8 ± 8.8	17.8 ± 0.7
Low-Ca pyroxene					
No. of points			5	5	1
SiO_2			58.3 ± 0.6	56.6 ± 1.8	56.5
FeO			0.90 ± 0.25	7.3 ± 5.0	10.8
Cr_2O_3			0.57 ± 0.27	0.64 ± 0.52	<0.04
MgO			37.1 ± 1.2	32.9 ± 3.5	31.4
CaO			1.4 ± 0.6	1.1 ± 0.7	0.72
Total			98.3	98.5	99.4
Fs (mol%)			1.3 ± 0.4	10.9 ± 7.5	16.0
Wo (mol%)			2.7 ± 1.0	2.1 ± 1.4	1.4

darkened H-chondrite clasts, and foreign CM carbonaceous-chondrite clasts. In addition, Plainview and Abbott contain carbon-rich aggregates (originally called graphite-magnetite aggregates by Scott et al. 1981a). Plainview also contains a few carbon-rich chondritic clasts related to the carbon-rich aggregates (Scott et al. 1981b; Rubin et al. 2005) and some light-colored unequilibrated chondritic clasts (Fodor and Keil 1976). Both Abbott and Plainview are shock-stage S3; they possess olivine grains that exhibit undulose extinction and contain small planar fractures (Stöffler et al. 1991).

Our data show that olivine in the Plainview host has a mean composition of Fa 17.8 ± 0.7 mol% (Table 1) and a range of Fa 16.3–20.2 (n = 47). The compositional distribution shows a sharp peak at Fa17–18, a shoulder at Fa 16 and a small ferroan tail extending to Fa 20.

Olivine in the Abbott host has a sharp peak at Fa 19–20, medium-size shoulders on both sides of the peak at Fa 18–19 and 20–21, a small, stumpy, ferroan tail extending to Fa 26–27 and a long magnesian tail extending to Fa 1–2 (Fig. 2 of Fodor et al. 1976).

Petrologic Characterization of CM Clasts

Clasts AB3 and AB8

These two clasts (AB3: 6400 × 640–1840 μm and AB8: 2060 × 1500 μm) form sharp boundaries with the Abbott host (Fig. 1). Both clasts contain olivine grains that exhibit undulose extinction and contain planar fractures, indicative of shock-stage S3.

The clasts contain minor magnetite, sulfide, Ca carbonate, Ca phosphate and accessory metallic Fe-Ni (Table 2). The sulfide in AB3 is pyrrhotite ($Fe_{1-x}S$) occurring as 2–10 μm size subrounded to subangular grains; sulfide in AB8 occurs as isolated 2–50 μm size grains of pyrrhotite and minor pentlandite [$(Fe, Ni)_9S_8$] and as rare sulfide-magnetite intergrowths, typically 10–30 μm in size. The metallic Fe-Ni in the clasts occurs mainly as small (1–10 μm) blebs within olivine phenocrysts inside chondrules.

Both clasts contain 30–35 vol% tochilinite-cronstedtite clumps, which are typically 30–50 μm in size. The tochilinite-cronstedtite intergrowths in AB3 have an average bulk compositional S/SiO_2 ratio of 0.01 and an "FeO"/SiO_2 ratio of 2.2; the intergrowths in AB8 have an average S/SiO_2 ratio of 0.03 and an "FeO"/SiO_2 ratio of 1.6 (Table 3). The mean analytical totals for the intergrowths in the two clasts are 85.0 and 87.1 (Table 3), indicating a significant amount of bound H_2O.

In clast AB8, clusters of magnetite blades occur within chondrule pseudomorphs; individual blades are typically 1–2-μm wide and 6–8 μm long. The magnetite clusters are quasi-equant and typically 20–90 μm across. Calcium carbonate grains in AB8 are surrounded by Mn-bearing carbonate.

Clast AB3 contains ~15 vol% porphyritic chondrules and chondrule fragments (80–200 μm in size) and isolated olivine grains (≤170 μm). Chondrule mesostases have been completely altered to phyllosilicate; ~15–20% of the mafic silicate phenocrysts in chondrules have also been altered (e.g., Fig. 2a).

Clast AB8 is distinctly yellow-green (i.e., spinach-colored) when viewed microscopically in plane-polarized transmitted light, indicating abundant phyllosilicate. The clast has experienced severe aqueous alteration; it contains ~25 vol% highly altered porphyritic chondrules (Figs. 6a and 6b); ~90% of the mafic silicate phenocrysts in these chondrules have been altered.

Chondrules in the two clasts are typical of those in CM chondrites (which average 270 μm in apparent diameter;

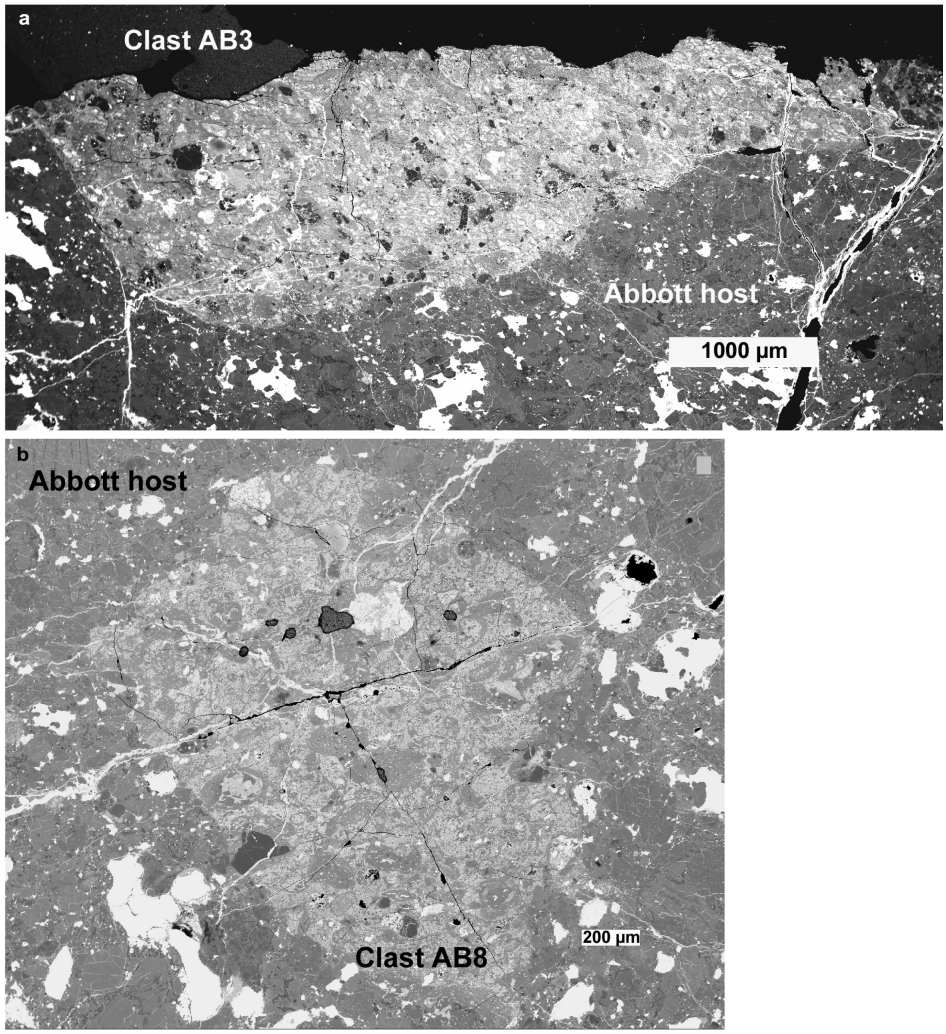

Fig. 1. Abbott clasts. a) Clast AB3 occurs at the edge of the thin section; its present size must be considered a lower limit. The clast forms a sharp boundary with the Abbott host. b) Clast AB8 is a highly altered CM chondrite that forms a sharp boundary with the Abbott host. Light-colored phases consist of magnetite and sulfide. Fractures (black) and veins of limonite [FeO(OH)] (white) that formed during terrestrial weathering penetrate the clast from the host. Backscattered electron (BSE) images.

Table 2. Modal abundances (vol%) of major phases in the CM clasts.

	AB3 type 2.3 ± 0.1	AB8 type 2.1	PV3 interior	PV3 rim
No. of points	348	191	160	72
Silicate*	95.7	91.6	91.2	88.8
Magnetite	0.6	2.1	1.9	0.01
Metal in chondrules	0.002	0.004	0.0003	0.0003
Sulfide	1.1	3.7	6.9	11.1
Limonite	2.6	2.6	0.0	0.0
Total	100.0	100.0	100.0	100.0

The metal abundances in the three clasts and the magnetite abundance in the PV3 rim were determined directly by measuring the surface area of each grain.
*Includes accessory Ca carbonate and Ca phosphate.

Rubin 2000). Most of the chondrules in the clasts are type-I; among the relatively rare type-II chondrules, many contain ferroan olivine phenocrysts with relict low-FeO cores.

Although few unaltered olivine grains remain in clast AB8, both clasts have similar olivine compositional distributions. In AB3, the distribution has a sharp peak at Fa 1–2, a small shoulder at Fa 0–1 and a broad tail extending to Fa 34 (Fig. 3a); in AB8 the distribution has a sharp peak at Fa 0–2 and a broad tail extending to Fa 33 (Fig. 3b).

We identified five refractory inclusions in AB3 (Fig. 4).

Table 3. Compositions (wt%) of tochilinite-cronstedtite (TC) intergrowths in clasts AB3 and AB8, and fine-grained matrix in the interior of clast PV3.

	AB3 (n = 26) TC intergrowths		AB8 (n = 36) TC intergrowths		PV3 matrix* (n = 50)
	Mean	Stdev	Mean	Stdev	Mean
SiO_2	21.8	6.4	25.9	2.3	43.1
TiO_2	0.06	0.03	0.09	0.02	0.14
Al_2O_3	2.4	0.75	3.3	1.2	3.6
Cr_2O_3	0.19	0.12	0.15	0.08	0.41
FeO	46.9	8.0	41.8	4.5	22.3
MnO	0.16	0.05	0.18	0.03	0.25
MgO	9.7	3.4	11.5	2.2	25.7
CaO	0.58	1.6	0.57	2.5	0.68
Na_2O	0.37	0.16	0.43	0.28	0.71
K_2O	0.04	0.02	<0.04	0.01	0.36
NiO	1.9	1.2	0.97	0.79	1.6
P_2O_5	0.43	1.5	0.54	2.6	0.10
S	0.19	0.15	0.68	0.50	0.85
Total	84.7		86.1		99.8
S/SiO_2	0.01		0.03		0.02
FeO/SiO_2	2.2		1.6		0.52

All Fe expressed as FeO.
*Matrix analysis from Table 1 of Fodor and Keil (1976); their Ni value of 1.3 wt% given here as 1.6 wt% NiO.

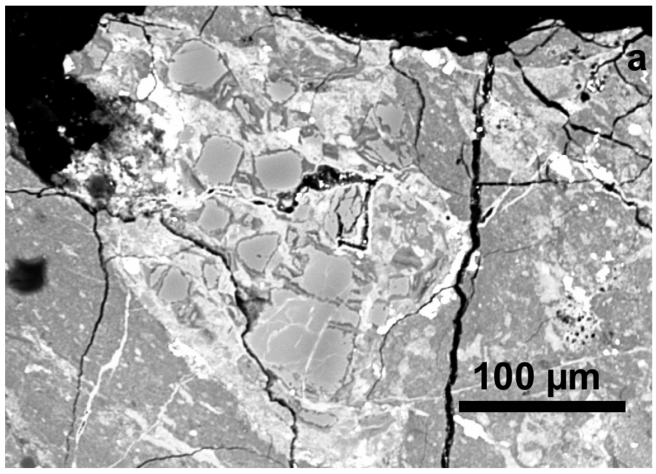

Fig. 2. Chondrules in clast AB3. A type-II (high-FeO) porphyritic chondrule containing altered ferroan olivine phenocrysts surrounded by phyllosilicate and sulfide. A dark mantle with a low modal abundance of opaque phases occurs around the chondrule. BSE image.

Three consist of spinel ($MgAl_2O_4$) and diopside ($CaMgSi_2O_6$) (e.g., CAI C2v; Fig. 4a) and two of diopside and phyllosilicate (e.g., CAI D2a; Fig. 4b). No refractory inclusions were identified in AB8.

Rubin et al. (2007) proposed a new aqueous alteration sequence for CM chondrites. The least-altered CM chondrite in their suite (Queen Alexandra Range [QUE] 97990) was assigned to petrologic subtype 2.6; the most-altered chondrites (e.g., LAP 02277; MET 01070), previously classified CM1, were assigned to subtype 2.0. Although there are some discrepancies, notably the very low metallic Fe-Ni contents of the clasts, subtypes can be assigned to the clasts: AB3 is subtype 2.3 ± 0.1 (comparable in its degree of aqueous alteration to QUE 99355 and Mighei); AB8 is subtype 2.1 (similar in texture to QUE 93005) (Rubin et al. 2007; Rubin 2007).

Clast PV3

PV3 (Fig. 7) consists of a 2250 × 1600 µm size clast interior (69 vol% in plane view) surrounded by a 10–500 µm thick rim (31 vol% in plane view). The clast interior plus rim assemblage is 2000 × 2800 µm. In three dimensions, the rim and the clast interior probably comprise subequal volumes. The shock stage of the clast (S3) is the same as that of the Plainview host (Stöffler et al. 1991).

The PV3 clast interior contains 1.9 vol% magnetite, 6.9 vol% sulfide and 0.0003 vol% metallic Fe-Ni (Table 2). Sulfide is present as pyrrhotite and minor pentlandite; metallic Fe-Ni occurs as rare 0.5–1 µm size blebs inside olivine phenocrysts in chondrules. Minor Ca carbonate surrounded by compositionally complex (Ca-, Mg- and Mn-bearing) carbonate also occurs.

Type-I porphyritic olivine (PO) and porphyritic olivine-pyroxene (POP) chondrules, 70–400 µm in mean diameter, are present. None of the low-Ca pyroxene phenocrysts exhibit polysynthetic twinning. Chondrule mesostases are fine grained and appear brown in plane-polarized transmitted light. Chondrule fragments range from 10 µm quasi-equant objects to elongated, 60 × 200 µm size fragments. One 240 × 320 µm isolated olivine grain with numerous fractures also occurs in the clast (Fig. 8a). The chondrules, fragments and isolated olivine grains constitute ~20 vol% of the clast interior; these objects are surrounded by fine-grained sulfide and sulfide-magnetite assemblages.

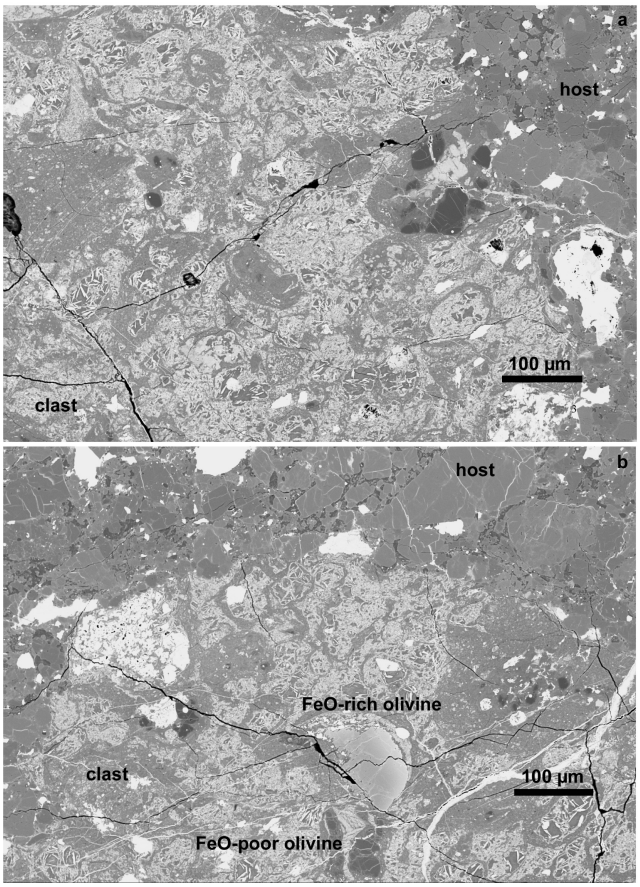

Fig. 3. Altered chondrules in clast AB8. a) Thin blades of magnetite (white) occur within chondrule pseudomorphs throughout the clast. Some chondrule pseudomorphs contain a few remnant mafic silicate phenocrysts (dark gray); others consist exclusively of magnetite and phyllosilicate. b) Remnant phenocrysts in highly altered chondrules. A large ferroan olivine grain (light gray) occurs near bottom center; FeO-poor olivine grains occur just below the ferroan grain. Thin magnetite blades are visible in chondrule pseudomorphs throughout the clast. Both a and b are BSE images.

Thin sulfide veins (0.2–0.5 µm × 10–50 µm) penetrate the chondrules, and, in many cases, completely surround the olivine and pyroxene phenocrysts (Fig. 8b). Many of the chondrules also contain 10–50 µm size magnetite-sulfide assemblages. Similar ~10 × 10 µm to 50 × 130 µm size assemblages, consisting of 60–90 vol% magnetite and 10–40 vol% sulfide, occur throughout the interior of PV3. Also present in the clast is a 10 × 400 µm magnetite-sulfide vein (Fig. 8c) and some ragged and elongated isolated sulfide grains.

Most chondrules, chondrule fragments and large isolated olivine grains are surrounded by silicate-rich, opaque-mineral-depleted patches similar in texture to the dark mantles around chondrules in CM chondrites (Metzler et al. 1992; Trigo-Rodríguez et al. 2006). Some mantle patches are thin rinds; others encompass twice the area of the enclosed chondrule or chondrule fragment in the plane of the section.

Olivine in the clast has a mean composition of Fa 2.0 mol% (Table 1) and a range of Fa 0.2–11.2. The olivine compositional distribution has a sharp peak at Fa 0–1, a broad shoulder at Fa 1–3 and a small tail extending to Fa 11 (Fig. 9a).

Two fragments of spinel-rich refractory inclusions (20 × 35 µm and 50 × 80 µm) are present; ~5 vol% of the larger fragment (CAI S6) consists of 2–3 µm diameter grains of perovskite ($CaTiO_3$) (Fig. 8a).

We confirm the observation by Fodor and Keil (1976) that phyllosilicates and tochilinite-cronstedtite do not occur in clast PV3. The mean analytical total of the fine-grained matrix of the clast is 99.8 wt% (Table 3; Fodor and Keil 1976), indicating that the matrix is basically anhydrous.

Rim around Clast PV3

Between the interior of the PV3 clast and its rim are discontinuous 50 × 250 µm size patches consisting of fine-grained (1–5 µm) sulfide grains enclosed in silicate melt material. The sulfide abundance in these patches is ~25 vol%; this is far higher than the average sulfide concentration in the interior (6.9 vol%).

The PV3 rim (Figs. 7, 8a, 8b, and 10) consists of 11 vol% sulfide, 89 vol% silicate (mainly fine-grained material, possibly devitrified melt), 0.01 vol% ~6 µm size magnetite grains, and 0.0003 vol% metallic Fe-Ni (occurring as very rare 2 µm diameter blebs embedded in olivine grains). Sulfide grains are typically 2–6 µm in size (although a few grains range up to 25 µm) and are elongated, irregular and ragged in shape.

The rim contains ~5 vol% relict, 8–60 µm size subrounded to subangular, mafic silicate grains (Fig. 10). Some of the olivine grains appear somewhat dark in transmitted light due to silicate darkening; these grains contain numerous 0.4–3 µm blebs of sulfide (e.g., Fig. 8d), as well as rare larger (~12 µm) sulfide grains. A few of the low-FeO olivine grains in the rim contain curved elongated sulfide veins (Fig. 8b).

Although the clast interior contains only type-I chondrules and chondrule fragments, the rim contains ~15% type-II chondrule fragments, some of which contain ferroan olivine phenocrysts with relict low-FeO cores. The rim's texture (Fig. 10) resembles that of a clast-laden impact-melt breccia (e.g., Apollo 16 sample 63503; Wilshire et al. 2007). No refractory inclusions occur in the rim.

Olivine in the PV3 rim has a mean composition of Fa 10.8 ± 8.8 mol% (Table 1) and a range of Fa 0.6–27.4. The olivine compositional distribution of the rim is bimodal: one peak is at Fa 1 with a tail extending to more ferroan compositions; the other peak is sharp and centered at Fa 18 (Fig. 9b). Approximately half of the olivine grains are in each mode.

Although the boundary between the PV3 rim and Plainview host is sharp, there are rare discontinuous patches consisting of 0.4–2 µm in diameter blebs of sulfide (~5 vol%)

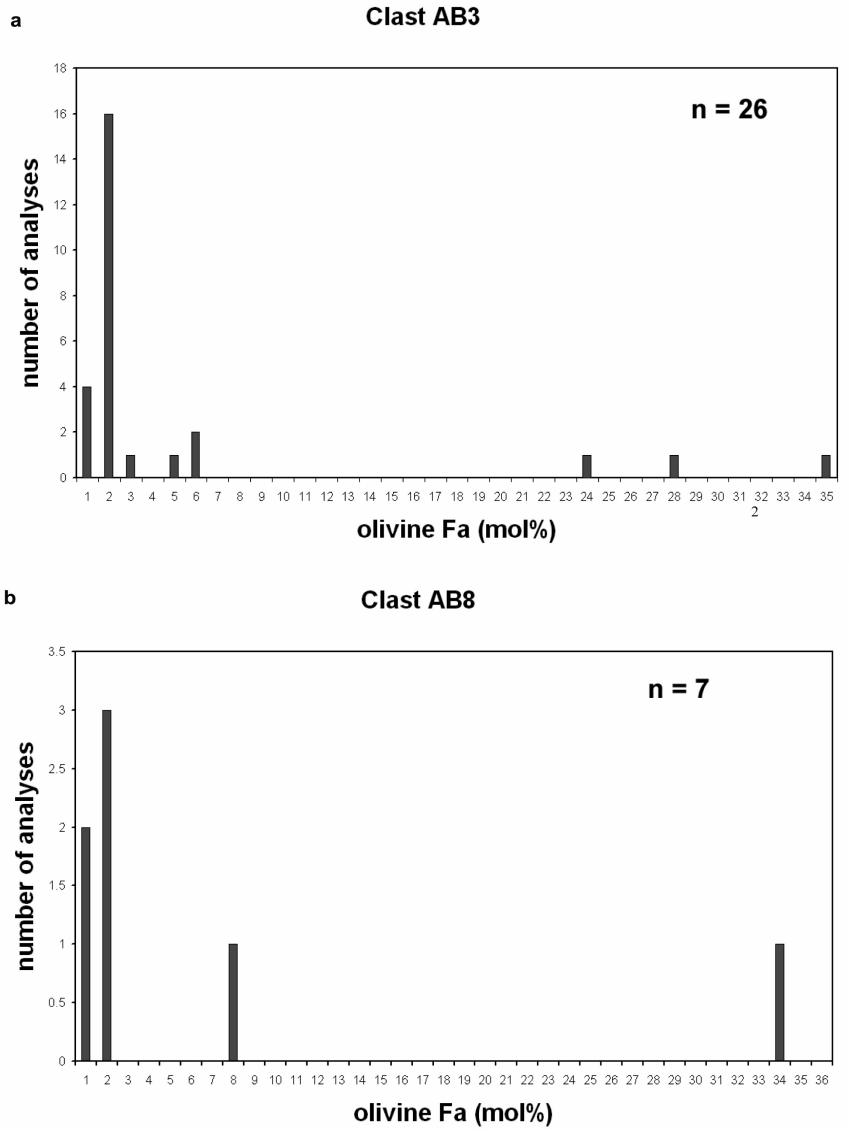

Fig. 4. Olivine compositional distributions in the Abbott clasts. a) Clast AB3 has a low-FeO peak and a ferroan tail extending to Fa 34. b) Clast AB8 has a low-FeO peak and a ferroan tail extending to Fa 33. The clast is so altered that few olivine grains remain that can be analyzed.

surrounded by quenched melt at the boundary (Fig. 11). The patches are 1–7 μm thick and ≤40 μm long.

DISCUSSION

Classification of the Clasts

Clasts AB3 and AB8

The dark-colored foreign clasts in Abbott and Plainview were recognized by Fodor and Keil (1976) and Fodor et al. (1976) as being type-II (i.e., CM) carbonaceous chondrites. Most of the clasts that they analyzed contain matrix phyllosilicates similar in composition and appearance (including having a green "spinach" color when viewed microscopically in transmitted light) to those in Murchison, a CM2 fall (Fuchs et al. 1973). The bulk water content of one clast in Abbott was measured directly by combustion techniques and found to be 9.38 ± 0.30 wt% (Table 11 of Fodor et al. 1976), similar to the amount of indigenous water (H_2O^+) in Murchison (8.95 wt%; Jarosewich 1990). The O-isotopic composition of one clast from Plainview ($\delta^{18}O = 6.5 \pm 0.1‰$), measured by Wilkening and Clayton (1974), is close to that of some individual CM chondrites (e.g., $\delta^{18}O = 6.38‰$ in ALH 83100; Clayton and Mayeda 1999). [The $\delta^{17}O$ content of the Plainview clast was not measured].

Like CM chondrites, the clasts contain carbonate and sulfide; AB3 and AB8 contain moderately abundant clumps of tochilinite-cronstedtite intergrowths as in many CM chondrites (e.g., Zolensky 1984; Tomeoka and Buseck 1985). Chondrules in the clasts have a mean apparent diameter in the range of 200–300 μm, similar to the mean in CM chondrites (270 μm; Table 2 of Rubin 2000).

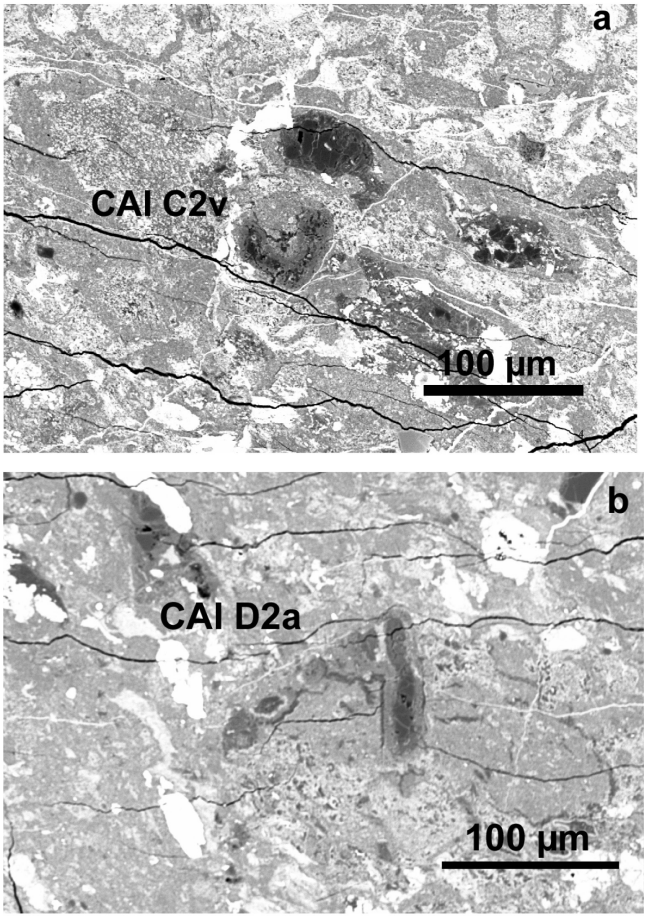

Fig. 5. Refractory inclusions in clast AB3. a) CAI C2v is a V-shaped inclusion fragment consisting of small grains of spinel (dark gray) and diopside (medium gray). b) CAI D2a is another V-shaped inclusion fragment; it consists of bands of diopside (medium gray) flanked by phyllosilicate (light gray). Both a and b are BSE images.

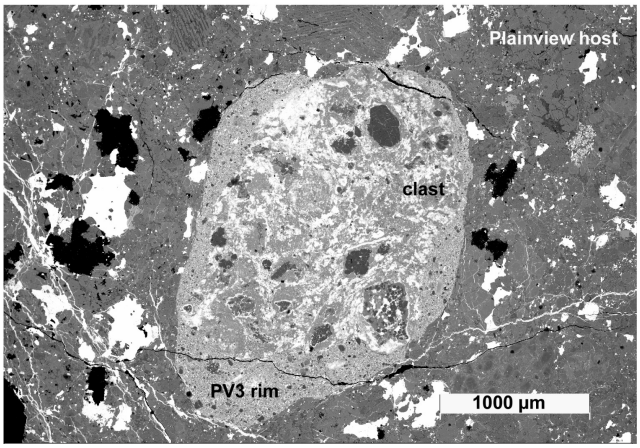

Fig. 6. Clast PV3 consists of a clast (interior region) and a melt rim. The rim forms a sharp boundary with the Plainview host. No tochilinite-cronstedtite or phyllosilicates occur in the PV3 clast or rim. Light-gray regions in the clast interior are mainly olivine; opaque phases (white) consist of magnetite and sulfide. BSE image.

It is clear that the clasts are fragments of CM-chondrite projectiles that were incorporated into the regolith of the H-chondrite parent body or perhaps into the regoliths of family members associated with the H-chondrite parent body. Clasts AB3 and AB8 do not exhibit shock effects more pronounced than those of the Abbott host. Both clasts contain abundant hydrous phyllosilicates and tochilinite-cronstedtite; they must have accreted to the H-chondrite regolith at sufficiently low relative velocities to avoid appreciable shock heating. The clasts were later weakly shocked by an unrelated impact event together with their host breccia.

Nevertheless, there are some modest mineralogical and compositional differences between the clasts and normal CM chondrites. Clast AB8 is somewhat richer in modal sulfide (3.7 vol%) than the modal sulfide abundance in CM chondrites measured by Rubin et al. (2007): 0.34–2.8 vol%. [The modal abundance of sulfide in clast AB3 (1.1 vol%) is within the normal CM range]. The S/SiO_2 weight ratios of tochilinite-cronstedtite in AB3 and AB8 (0.03 ± 0.02 and 0.01 ± 0.01, respectively) are somewhat below the range for normal CM chondrites (0.05–0.35; Table 3 of Rubin et al. 2007).

With progressive aqueous alteration, tochilinite-cronstedtite in CM chondrites develops lower S/SiO_2 ratios, reflecting an increase in the tochilinite-cronstedtite phyllosilicate/sulfide ratio (Rubin et al. 2007). Loss of S from tochilinite-cronstedtite is attended by the formation of relatively coarse sulfide grains and an increase in the whole-rock modal sulfide abundance. The high bulk modal sulfide abundance and the low S/SiO_2 ratios in tochilinite-cronstedtite in the clasts are consistent with the trend in CM chondrites, but are somewhat outside the nominal range.

Clast PV3

The absence of phyllosilicates in clast PV3 indicates that it is not a normal CM chondrite. Nevertheless, there are several properties that suggest that it was derived from a CM projectile:

1. With the exception of phyllosilicates, the major and minor minerals in the clast (olivine, low-Ca pyroxene, pyrrhotite, pentlandite, magnetite, metallic Fe-Ni, Ca carbonate) are the same as those in typical CM chondrites.
2. The olivine compositional distribution of the clast interior (Fig. 9a) is very similar to that of olivine grains in chondrules from the Murchison CM fall (Fig. 10 of Fuchs et al. 1973) as well as the distributions in the CM clasts in Abbott (Fig. 3). Each distribution has a large peak at very low Fa contents and a low flat tail extending to higher Fa values.
3. The major-element bulk composition of clast PV3 is very similar to that of CM2-chondrite falls calculated on a water-free basis (Table 4). For example, the SiO_2, FeO

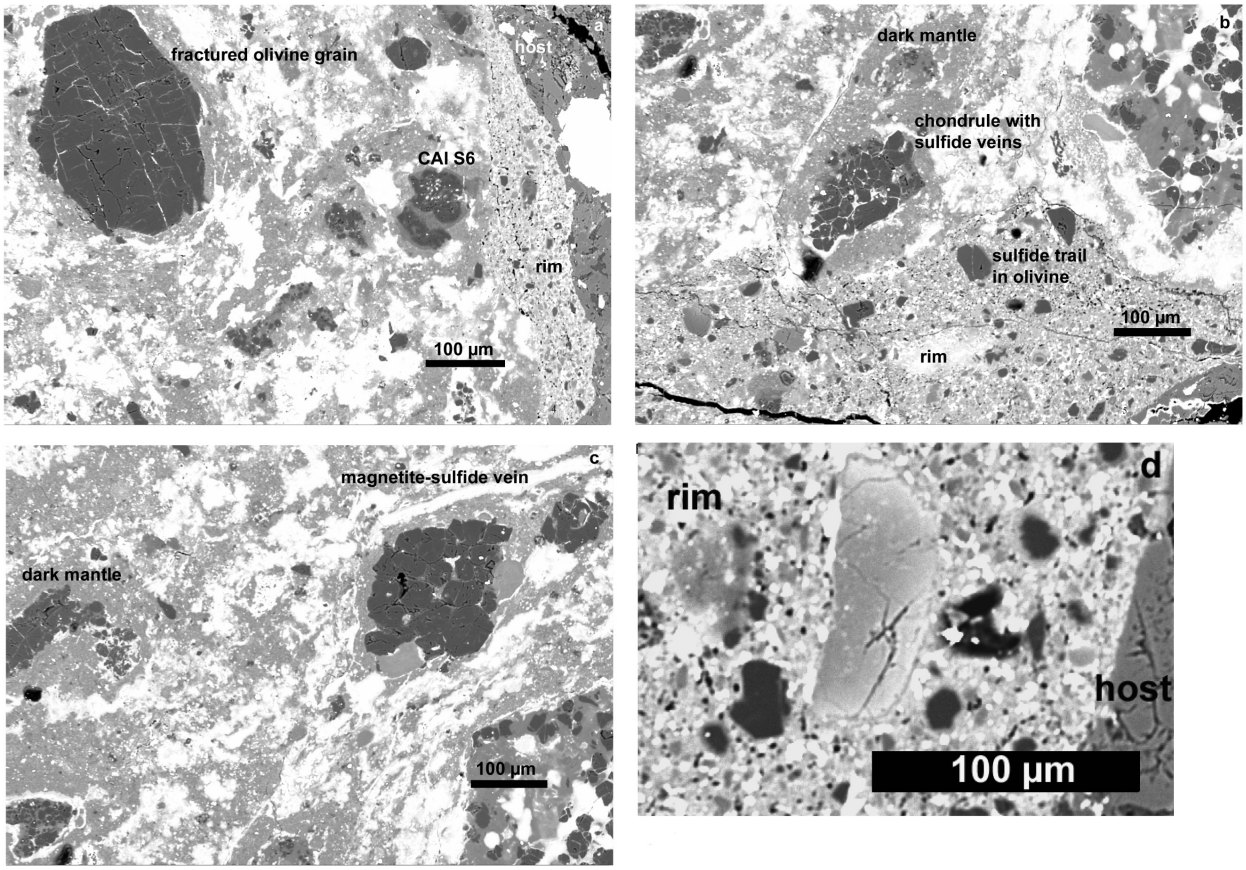

Fig. 7. Selected petrographic features of clast PV3. a) Large isolated low-FeO olivine grain (upper left) with numerous fractures, many filled by thin veins of sulfide. CAI S6 occurs at the right margin of the clast. The CAI consists of spinel (dark gray) enclosing small blebs of perovskite (white). The rim at right contains numerous small grains of sulfide (very light gray) and mafic silicate (medium to dark gray). b) Thin sulfide veins surround the phenocrysts of a type-I (low-FeO) chondrule (left of center). The chondrule is surrounded by an extensive dark mantle containing a relatively low abundance of opaque phases. A low-FeO olivine grain near the top of the rim (center of image) is bisected by a thin quasi-linear trail composed of small sulfide blebs. c) Elongated magnetite-sulfide vein (top right) extending beyond the image for a total length of 400 µm; it is located just above a low-FeO chondrule. d) Ferroan olivine grain in rim that exhibits silicate darkening; the grain contains many small blebs of sulfide. All four figures are BSE images.

and MgO concentrations in the clast and in normalized-CM chondrites are (in wt%): 33.4 and 33.3, 33.9 and 32.0, and 23.3 and 22.8, respectively. The concentrations of many of the minor components (TiO_2, Al_2O_3, Cr_2O_3, MnO, CaO and NiO) in PV3 and normalized CM chondrites are almost identical (Table 4).

4. The three apparently intact chondrules in the clast have an average apparent diameter of 280 ± 130 µm, very similar to that of mean CM chondrules (~270 µm; Table 2 of Rubin 2000). All of the chondrules in the PV3 clast are low FeO; these chondrules are the most common type in CM chondrites. Most chondrules in PV3 are surrounded by opaque-mineral-depleted rims that resemble the dark mantles of matrix material around chondrules in CM-chondrite whole rocks (Metzler et al. 1992; Trigo-Rodríguez et al. 2006).
5. The refractory-inclusion fragments in PV3 are spinel rich; spinel-rich objects are the most common type of refractory inclusion in CM chondrites (e.g., Greenwood et al. 1994; MacPherson and Davis 1994; Simon et al. 2006; Rubin 2007).

If PV3 was a normal CM chondrite prior to colliding with the Plainview regolith (as argued here), it would most likely have contained phyllosilicates and tochilinite-cronstedtite. The decomposition of serpentine requires temperatures in excess of ~700 °C (Fig. 2 of Akai 1990). The absence of phyllosilicates is consistent with the model that impact heating was responsible for dehydration of the clast. Another indicator of heating exhibited by the clast is the absence of polysynthetically twinned low-Ca clinopyroxene grains (which are normally present in CM-chondrite whole rocks). [Low-Ca clinopyroxene transforms into orthopyroxene at temperatures ≥630 °C (Boyd and England 1965; Grover 1972)].

There are examples of other chondritic projectiles that experienced impact heating when they accreted to their host regoliths. Bench Crater is a 1.5 × 3 mm size CM chondrite that suffered partial dehydration during impact to the lunar

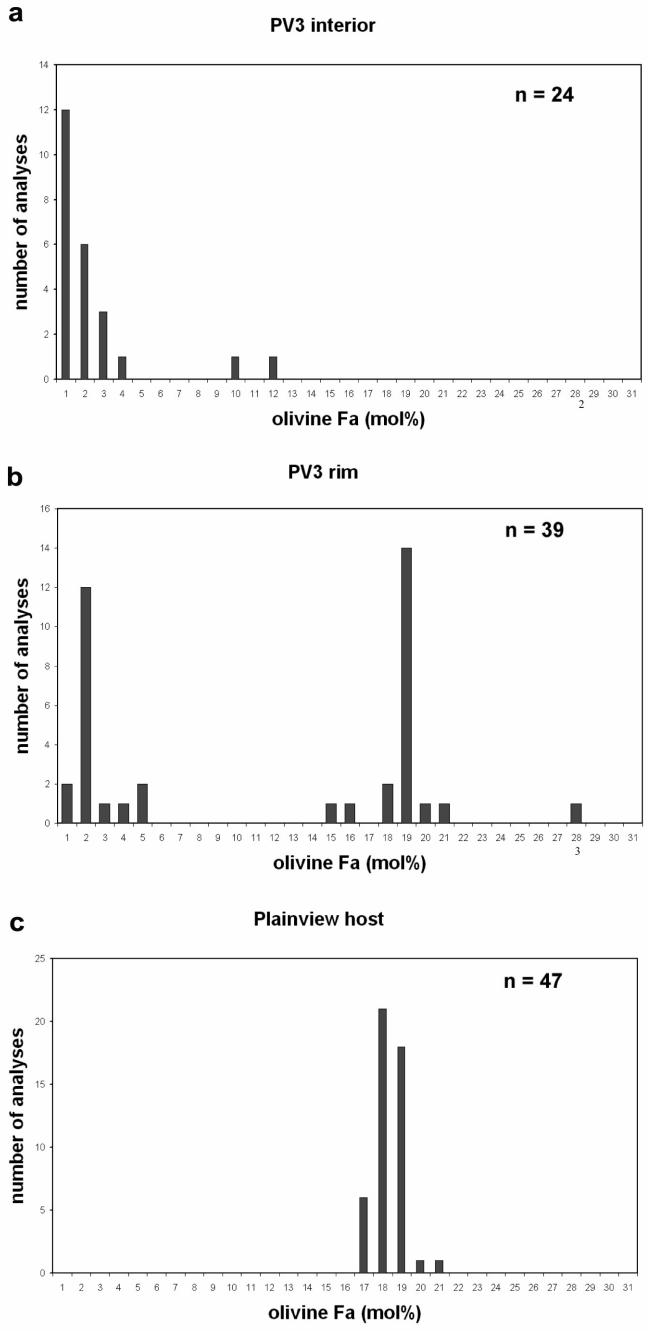

Fig. 8. Olivine compositional distributions in the Plainview clast, rim and host. a) Olivine in the PV3 clast interior has a low-FeO peak and a short tail extending to Fa 11. b) Olivine in the rim exhibits a bimodal distribution. Peaks occur at Fa 1 and Fa 18; subequal numbers of olivine grains occur in each mode. The distribution in the rim appears to be a roughly equal mixture of olivine from the clast and the host. c) Olivine in the Plainview host has a relatively broad, high-FeO peak at Fa17–18.

regolith (McSween 1976; Zolensky 1997); Hadley Rille is a 1.1 × 1.2 mm size EH chondrite that was partly melted when it accreted to the lunar regolith (Haggerty 1972; Rubin 1997b). The heating of these clasts is likely related to the host projectile's impact velocity, which could be no smaller than

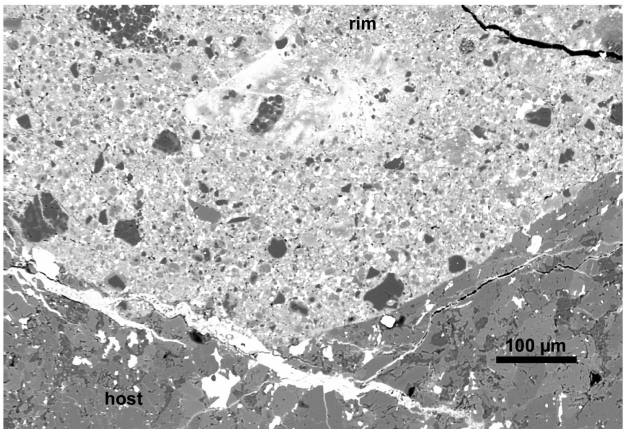

Fig. 9. Texture of the PV3 rim. The rim contains angular fragments of low-FeO and high-FeO olivine grains (gray) and small sulfide grains (white) enclosed by a fine-grained (or glassy) quenched silicate melt. Similar textures occur in lunar clast-laden impact-melt rocks. BSE image.

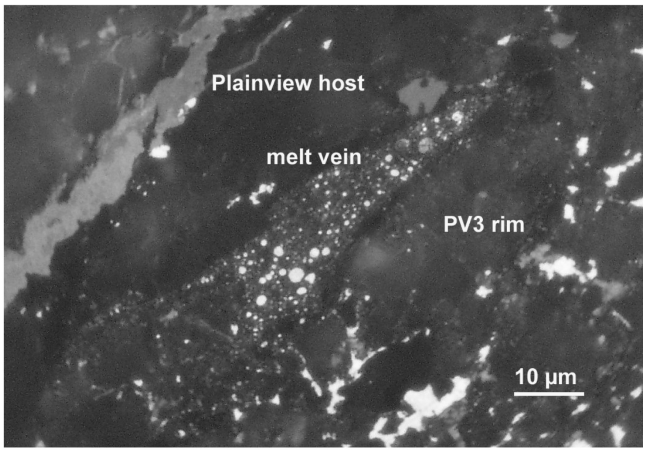

Fig. 10. Melt vein at boundary between the PV3 rim and the Plainview host containing numerous small blebs of sulfide (white). White grains in the rim (right) are also sulfide; light-gray vein in the host (left) running NE-SW is limonite, a product of terrestrial weathering. Reflected light image taken with an oil-immersion objective lens.

the lunar escape velocity combined with that of the Earth's at lunar distance (2.78 km/s). While these velocities are high enough to shock and melt a considerable amount of a projectile, numerical impact simulations indicate that a significant fraction escapes shock pressures >10 GPa (Bland et al. 2008). Still, the paucity of unshocked meteorite clasts among lunar samples, despite evidence that 1–2% of the lunar regolith is made of up meteoritic material (e.g., Wasson et al. 1975; McKay and Warren 1991), indicates that the conditions needed to create unshocked clasts in lunar regolith breccias similar to the AB3 and AB8 either do not happen very often or they exist in regions yet to be sampled.

A few carbonaceous chondrite whole rocks exhibit mineralogical, petrologic, and chemical properties that resemble CM chondrites, but contain only rare phyllosilicates

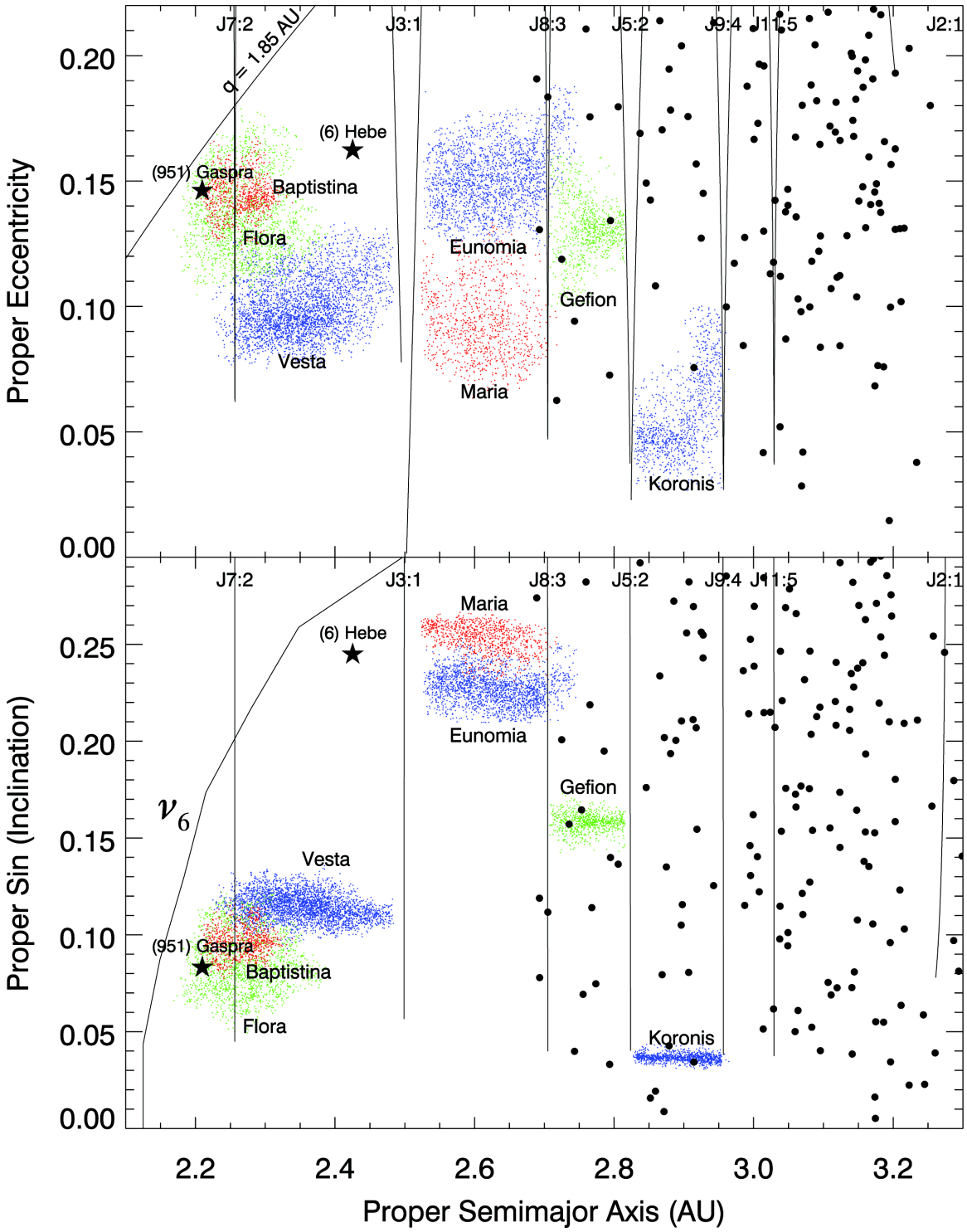

Fig. 11. The location of the asteroid resonances, asteroid families, individual asteroids, and other objects described in the text in semi major axis, eccentricity, and inclination space. The mean motion resonances with Jupiter (designated by the letter J), are taken from Nesvorný et al. (2002), while the location of the υ6 secular resonance is from Bottke et al. (2002). The data for prominent asteroid families Baptistina, Eunomia, Flora, Gefion, Maria, and Vesta are from D. Nesvorný (personal communication). The data for individual asteroids is from the AstDys website of A. Milani et al. (http://hamilton.dm.unipi.it/astdys/). The black dots started from 2.6 AU are the orbital parameters of the model comets embedded onto stable orbits within the main belt by the dynamical events described by the Nice model (see Levison et al. 2009). These objects are a probable source for the CM clasts described in the text, provided the clasts are 3–4 Ga old. On the other hand, if the CM clasts are less than 200 Ma old, a probable source is the Baptistina family located adjacent to the Flora and Vesta families in the inner main belt.

Table 4. Bulk composition of clast PV3 compared to CM chondrite falls (calculated on a water-free basis).

	PV3 bulk[§]	CM2 falls[*] normalized to 100 wt%
SiO_2	33.4	33.3
TiO_2	0.16	0.15
Al_2O_3	2.3	2.5
Cr_2O_3	0.49	0.49
FeO	33.9	32.0
MnO	0.26	0.29
MgO	23.3	22.8
CaO	2.3	2.2
Na_2O	0.33	0.49
K_2O	0.20	0.07
NiO	1.8	2.0
P_2O_5	0.21	0.28
S	3.0	3.6
Total	101.6	100.2
S/SiO_2	0.09	0.11
FeO/SiO_2	1.0	0.96

[§]Bulk analysis from Table 2 of Fodor and Keil (1976); their Ni value of 1.4 wt% reported here as 1.8 wt% NiO.

[*]CM2 data are from Jarosewich (1990). Data were omitted for H_2O, C, CoO and CO_2 and normalized to 100 wt%; Ni expressed as NiO; all Fe is expressed as FeO.

(e.g., Y-86720; Tomeoka et al. 1989). Instead of phyllosilicates inside chondrules, there are silicate materials (characterized as "chondrule replacement products") in Y-86720 that have high analytical totals, indicating that little bound water is present. Such rocks were probably thermally metamorphosed and dehydrated CM chondrites (Tomeoka et al. 1989). We speculate that the heating experienced by these rocks was caused by impact processes.

Formation of the Rim around PV3

The olivine compositional distribution in the rim around clast PV3 appears to be the result of nearly equal mixing of material from the Plainview host (which has a peak at Fa 17–18; Fig. 9c) and the clast interior (which has a peak at Fa 0–1; Fig. 9a). In order to test whether the rim could have been derived from a nearly equal mixture of CM clast material and H-chondrite host, we averaged analyses of two different 100 × 100 μm portions of the rim located on opposite sides of the clast. The rim shows some point-to-point variability, mainly reflecting different proportions of silicate and sulfide. The bulk composition of the rim (Table 3) is not very different from the major-element bulk compositions of either CM2 or H-chondrite falls (normalized to 100 wt%) determined by Jarosewich (1990). The rim composition is thus also similar to a hypothetical 50:50 mixture of CM- and H-chondrite material (Table 3).

The low-FeO peak in the olivine compositional distribution of the rim of clast PV3 (Fig. 9b) does not exactly match the peak in the clast interior (Fig. 9a): the clast's peak is at Fa 0–1, whereas the low-FeO peak in the rim is at Fa 1–2. Nevertheless, the low-FeO peak in the rim closely matches the peak of clast AB3 (Fig. 3a). This suggests that the olivine compositional distribution in the interior of clast PV3 may have initially resembled the distribution in clast AB3, but was modified after accretion of the clast to the H-chondrite regolith. This most likely involved minor reduction during annealing, moving the PV3 peak from Fa 1–2 to Fa 0–1.

The ferroan tail of the olivine compositional distribution in clast AB3 extends to Fa 34 (Fig. 3a), that of clast AB8 to Fa 33 (Fig. 3b), and that of isolated olivine grains in Murchison to Fa 58 (Fig. 10 of Fuchs et al. 1973). This suggests that the progenitor of clast PV3 initially may also have had an extended ferroan tail and that the single Fa 27 grain analyzed in the PV3 rim was derived from the clast and not from the Plainview host (where such ferroan, compositionally aberrant grains are very rare).

Olivine grains in the Plainview host have a broader peak (Fa 17–18; Fig. 9c) than the high-FeO peak in the PV3 rim (Fa 18; Fig. 9b). This difference may reflect partial equilibration of the (small) olivine grains in the PV3 rim during annealing.

Although clast PV3 does not presently exhibit more significant shock effects than the Plainview host (both are stage S3), the occurrence of some olivine grains with significant darkening in the PV3 rim (e.g., Fig. 8d) suggests that the PV3 clast was once shocked to a higher stage and later mildly annealed (cf. Rubin 2004). A higher prior shock history is also consistent with the occurrence of veins of sulfide in the chondrules in the PV3 clast interior (Fig. 8b) and with an elongated magnetite-sulfide vein that transects the clast (Fig. 8c).

The bimodal olivine compositional distribution of the PV3 rim is consistent with a model in which the rim formed from an impact melt that consisted of about equal proportions of Plainview regolith material and a CM projectile. We suggest that clast PV3 was initially part of a normal CM projectile that accreted to the H-chondrite regolith at a moderate relative velocity and became appreciably shocked. Upon impact, this CM projectile was shocked, dehydrated, partly melted, and fragmented. The PV3 clast formed from a fragment of the projectile that was engulfed in a melt mixture of the projectile and the target. The PV3 rim is thus somewhat analogous to the agglutinate-like rim that surrounds the Hadley Rille enstatite chondrite (Fig. 1 of Rubin 1997b); the latter rim was formed during collision of the Hadley Rille projectile with the lunar regolith.

During collisional heating of PV3, metallic Fe-Ni and sulfide in the clast melted and was injected through fractures in adjacent silicate grains, causing darkening (Rubin 1992). Olivine grains in the clast were damaged; presumably, they developed undulose extinction, planar fractures, and possibly mosaicism.

The impact event produced silicate melt (the present rim) that engulfed the clast. Annealing of the clast caused the phyllosilicates in the clast to dehydrate and the olivine crystal

Table 5. Bulk composition of the PV3 rim (wt%).

	PV3 rim*	PV3 rim (n = 200)	mean PV3 rim	H falls	50:50 mixture of CM and H	
	Mean	Mean	St dev	Normalized to 100 wt%	Normalized to 100 wt%	Normalized to 100 wt%
SiO_2	34.5	33.7	5.2	34.4	35.6	34.8
Al_2O_3	2.5	2.8	1.4	2.9	2.1	2.3
Cr_2O_3	0.47	0.49	0.67	0.50	0.51	0.51
FeO	32.1	31.6	7.0	32.2	34.4	33.6
MnO	0.26	0.25	0.07	0.26	0.30	0.30
MgO	21.7	22.9	6.4	23.3	22.6	22.9
CaO	2.3	2.4	1.4	2.4	1.7	2.0
Na_2O	0.41	0.64	0.38	0.65	0.84	0.67
K_2O	0.12	0.07	0.04	0.07	0.09	0.08
S	2.5	3.2	4.0	3.3	1.9	2.8
Total	98.4	98.0		100.0	100.0	100.0

*Rim composition from Table 2 of Fodor and Keil (1976) determined by broad-beam electron microprobe techniques; they also reported 0.12 wt% TiO_2, 0.22 wt% P_2O_5 and 1.2 wt% Ni.The composition of the rim determined in this study was derived from electron-microprobe analysis using a 6 μm diameter beam and combining the analyses of two 100 × 100 μm grids located on different sides of the PV3 clast. CM2 data from Table 4 was used in conjunction with H-chondrite data from Jarosewich (1990). All Fe is expressed as FeO.

lattices to heal (e.g., Bauer 1979; Ashworth and Mallinson 1985). Some of the evidence of the clast's prior thermal history was erased during this annealing event. It seems likely that, after annealing, olivine grains would have exhibited sharp optical extinction, characteristic of an unshocked rock of stage S1. (Members of several meteorite groups have apparently experienced post-shock annealing; these include many equilibrated ordinary chondrites [Dixon et al. 2004; Rubin 2004], EL6 chondrites [Rubin et al. 1997], CK4–6 chondrites [Rubin 1992], and ureilites [Rubin 2006]).

After the clast cooled, additional impacts into the Plainview regolith caused PV3 to become weakly shocked along with the rest of the adjacent H-chondrite regolith material (i.e., the Plainview host).

Plainview also contains a light-colored, 4 × 1.5 cm size, 3.63 Ga old impact melt rock clast of H-chondrite parentage (Keil et al. 1980). This clast forms a sharp boundary with the Plainview host. It seems very likely that this clast formed from H-chondrite regolith material by the impact of a projectile (of unknown composition) into the regolith. The occurrence of this clast in Plainview might mean that the Plainview region of the H-chondrite parent-body regolith was active 3.63 Ga ago. Alternatively, it is possible that the clast formed in another surface region of the H-chondrite parent body at this time and was incorporated long after its formation into the Plainview region of the regolith by another impact event (Keil et al. 1980). The melt-rock clast thus cannot be used to date definitively the time the progenitor of PV3 accreted to the H-chondrite parent body.

Low-Velocity Accretion of CM Projectiles to H-chondrite and HED Regoliths

The two clasts in Abbott exhibit appreciably different degrees of aqueous alteration (AB3 is type 2.3 and AB8 is type 2.1). Although it is possible that they were derived from a single brecciated projectile that contained clasts that experienced different degrees of aqueous alteration (cf. Rubin and Wasson 1986), it is more probable that they were derived from separate projectiles, each of which was characterized by distinctive and essentially uniform degrees of alteration. This would be consistent with the petrologic characteristics of CM Murchison; different thin sections of this meteorite exhibit very similar degrees of alteration (e.g., Rubin et al. 2007).

Wilkening (1973) and Wilkening and Clayton (1974) recognized that the presence of phyllosilicates in CM clasts in H chondrites and in HED breccias required that the progenitors of the clasts were projectiles that collided with their hosts at low relative velocities (see also Gounelle et al. 2003). Otherwise, appreciable shock-heating would have occurred and the clasts would likely have dehydrated, as was apparently the case for PV3.

During the impact of a CM projectile to a foreign parent asteroid, *small amounts* of relatively unshocked material could be spalled off the rear of the projectile and survive as centimeter-size clasts. Some of the spalled material could achieve a low velocity relative to the surface of the asteroid (Melosh 1989; see also Bland et al. 2008). It is possible that clasts AB3 and AB8 formed this way. These clasts may have been delivered by smaller projectiles, although that formation scenario requires particular conditions that will be discussed below.

There are many hydrated, relatively unshocked clasts in H-chondrite regolith breccias; they occur in Plainview (Fodor and Keil 1976), Abbott (Fodor et al. 1976), Leighton (Wilkening 1976), Tysnes Island (Keil and Fodor 1980), and Ipiranga (Rubin 1982). MacPherson et al. (1993) described one such clast in the Magombedze H3–5 chondrite breccia. Relatively unshocked CM clasts are also present in various HED breccias (e.g., Wilkening 1973; Bunch et al. 1979;

Kozul and Hewins 1988; Pun 1992; Brearley 1993; Buchanan et al. 1993; Zolensky et al. 1992; Zolensky et al. 1996; Gounelle et al. 2003). These objects provide additional constraints on the provenance of the CM clast progenitors.

CM-like Clasts in the Asteroid Population and the Inner Solar System

Before we can evaluate formation scenarios for the presence of unshocked and lightly shocked CM clasts in the H and HED meteorite classes, we need to discuss what is known about CM-like material in the asteroid belt and inner solar system.

First, CM clasts appear to be relatively common in H and HED regolith breccias and are rare to absent in other meteorite types. In HED breccias, Zolensky et al. (1996) found that 83% of the foreign clasts are CM and ~15% are CR; Gounelle et al. (2003) found that ~50% of the clasts are CM and ~50% are CR. Unshocked CM clasts similar to the AB3 and AB8 clasts described above have been found only in the H and HED meteorite classes. Some CM clasts similar to PV3 apparently arrived at velocities high enough to be shocked and dehydrated but not high enough to be vaporized. In general, dark carbonaceous chondrite-like clasts in other meteorite classes (e.g., CV3 chondrites; Kracher et al. 1985; see references in Wasson and Wetherill 1979) are a poor match to known CM meteorites. It is unclear whether a selection bias exists.

The proportions of H chondrites and howardites that are regolith breccias (15.3% and 38.1%, respectively) are higher than those in L or LL chondrites (3% and 5.5%, respectively), but are lower than or roughly comparable to those in other chondrite or achondrite classes (e.g., E: 9.6%; R: 47.8%; aubrites: 30%; ureilites: 12%) (Bischoff et al. 2006).

Second, if we assume that CM clasts were not spall from a larger projectile, the progenitors of some CM clasts were delivered to the surface of the target asteroids at very low relative velocities. The precise impact velocity needed to avoid dehydrating small CM-type projectiles is unknown. Gounelle et al. (2003) argued that small projectiles striking asteroids at velocities ≤1000 m s^{-1} may allow some fragments to survive, but it is unclear whether these materials would also avoid dehydration. In all likelihood, impact speeds below several hundreds of m s^{-1} (say, ≤300 m s^{-1}; e.g., Fig. 1 of Hartmann 1979; Fig. 1 of Bischoff et al. 2006) give projectiles the best chance of avoiding significant shock.

Interestingly, this constraint raises problems for delivery scenarios that assume that CM clasts come from small, low-velocity projectiles. It is currently believed that the H and HED parent bodies were 200–500 km in diameter (with the HED parent body plausibly being 4 Vesta (Keil 2002; e.g., Treiloff et al. 2003). The escape velocity for such large objects, assuming bulk densities comparable to those found in ordinary chondrites and the HED meteorites (Britt et al. 2002), should be 140–350 m s^{-1}. This means that even if the CM clast progenitors, which presumably were centimeter-size, had nearly identical orbits to the H and HED parent bodies, they would still have little to no chance of landing at ≤300 m s^{-1}.

On the other hand, this particular mechanism can still work if the following conditions are true: (i) small CM projectiles happened to strike genetically related family members of the H and HED parent bodies; these bodies would have low enough escape velocities that very low impact velocities would be possible, (ii) the family members of the H and HED parent bodies happen to produce large quantities of the regolith breccia meteoroids falling on Earth today, and (iii) the H and HED parent bodies had sizable asteroid families when the CM projectile flux was high.

Third, there is evidence from lunar soils that CM- or CI-like material has been common in the inner solar system for the last 3.9 Ga. Uncontaminated lunar crust is known to have very low concentrations of siderophile elements; thus, the siderophiles in lunar crustal materials are thought to have been delivered mainly by micrometeorite impacts. Using siderophile-element/Ir ratios, Wasson et al. (1975) estimated that the lunar regolith contains 1–4 wt% of debris implanted by primitive, volatile-rich carbonaceous chondrites (see also Haskin and Warren 1991). This material resembles portions of the micrometeorite population striking Earth today and may be closely related to CM or CI chondrites. Regolith samples taken from various Apollo sites also indicate that the influx of this material was at least a factor of four higher between 3.7–3.9 Ga ago (Apollo 14, 16, 17 samples) than it has been over the last 3.5–3.2 Ga (Apollo 12, 15 samples) (Wasson et al. 1975). The source of this material is unknown but is likely to be comets and/or primitive asteroids.

Meteorite Delivery from the H and HED Parent Bodies

We can use the properties above to consider various CM-clast delivery scenarios, provided we understand the meteorite delivery process (see Bottke et al. [2006] for a recent review). We start our discussion with the delivery of H chondrites to the Earth, a subject that has received considerable attention in the literature.

Although it is possible that H chondrites come from more than one parent asteroid, ~45% of them have cosmic-ray-exposure (CRE) ages that fall within a single peak centered at 7–8 Ma (Graf and Marti 1995). This indicates that these particular samples were derived from the same kilometer- or multi-kilometer-size region on a single body (Anders 1978). For the sake of simplicity, we assume that all of the H chondrites have the same provenance.

In the 1990s, several papers (Farinella et al. 1993; Migliorini et al. 1997; Gaffey and Gilbert 1998) argued that the probable source of the H chondrites was 6 Hebe, a ~200 km asteroid with osculating semimajor axis a, eccentricity e, and inclination i values of 2.42 AU, 0.20, and 14.8°, respectively (Fig. 11). These workers favored Hebe over other candidate

asteroids because (i) Hebe has the right spectroscopic signature to be a candidate source for ordinary chondrites, being of taxonomic class S (IV), (ii) it is located near the υ6 secular resonance and 3:1 mean motion resonance with Jupiter (J3:1), both important transportation routes for delivering material to the Earth (see below), and (iii) Hebe is sufficiently large that frequent cratering events on its surface could directly inject meteoroid-sized debris into the υ6 and J3:1 resonances. At the time these papers were written, direct injection of material into resonances via collisions was seen as the most viable means for delivering asteroids and meteorites to the planet-crossing region.

The problem with the direct injection scenario for H chondrites (and other meteorites) is that it produces results that are inconsistent with the constraints provided by main-belt asteroids, near-Earth asteroids, and meteorites (cf. Bottke et al. 2006). For example:

- Most stony meteorites have CRE ages between 10 and 100 Ma, whereas direct-injection models predict that most objects should have CRE ages less than a few Ma, the typical dynamical lifetime of objects in the inner solar system (e.g., Gladman et al. 1997; Bottke et al. 2002). This strongly suggests that direct injection is, at best, a sporadic mechanism for producing stony meteorites.
- The ejection velocity distributions used by the direct-injection models to launch material into resonances (e.g., Farinella et al. 1993) were skewed to high values that are inconsistent with data from both laboratory shot experiments and numerical hydrocode experiments. The reason these values were skewed is that they were taken from the orbital spreads of family members in asteroid families. It is now known that these spreads have been heavily influenced by Yarkovsky thermal forces (Bottke et al. 2001).
- Cratering events on Hebe capable of injecting small fragments into resonances should also produce larger, observable asteroidal fragments near the target body. To date, no cluster of fragments (i.e., a minor asteroid family) has been found near Hebe (Nesvorný et al. 2003). Moreover, our understanding of the main belt population (e.g., Jedicke et al. 2002) indicates there are insufficient projectiles capable of supporting a steady-state population of meteoroids from Hebe via collisional injection alone.

Based on all these factors, we consider it unlikely that Hebe is the main H-chondrite parent body.

More modern meteorite delivery models show that most meteoroids reach Earth through a process involving collisional events on their precursor bodies as well as by a number of slow-working dynamical processes. Insights into these processes have been gleaned from numerical models that attempt to account for the collisional and dynamical evolution of the asteroid belt over the last 4.5 Ga (e.g., Bottke et al. 2005a, 2005b, 2005c, 2006a, 2006b). Collisional and dynamical modeling indicate that meteorite groups that produce numerous falls (e.g., L, H, HED, LL, CM; Grady 2000; Burbine et al. 2002) are more likely to be derived from asteroid families than from individual objects (Bottke et al. 2005c). When an asteroid is hit by a projectile, a fragment size distribution (FSD) is produced. For the purposes of discussion, we assume here that the FSD is large enough to include both meter-size bodies (meteoroids) as well as larger objects (asteroids).

If the original parent asteroids were relatively homogeneous, subsequent collisions onto bodies in the FSD act as a source for new meteoroids that are genetically the same as those created in the previous generation. These sequential fragmentation processes are called collisional cascades and they guarantee that meteoroids from the original parent body will be provided to the main-belt population for some time after the initial impact event. In fact, if the reservoir of new material is large enough, a family can literally dominate the local background population for timescales of hundreds of Ma to several Ga after the original breakup event occurred.

At the same time, dynamical processes such as the Yarkovsky effect (e.g., Peterson 1976; Bottke et al. 2002a, 2006b) and resonances (e.g., Bottke et al. 2002b) push meteoroids and larger bodies out of the main belt, while collisions can act as sinks to eliminate meteoroids entirely. Thus, after the initial family-forming event, the sources and sinks, over some time interval, will drive the meteoroid population from a family toward a quasi-steady state. If the sink processes dominate the sources, the meteoroid population will undergo decay as collisions affect the FSD by depleting the reservoir of larger bodies capable of replacing the population. This means that the size and nature of the FSD determine the size and decay rate of the meteoroid population, while the quantity of meteoroids reaching the Earth is controlled by the efficiency of the main-belt escape hatches near the FSD at producing Earth impactors.

For the latter, Bottke et al. (2006a) tracked the dynamical evolution of test bodies placed in various main-belt resonances and determined the fraction that hit the Earth. They found that test bodies escaping the main belt from resonances with a <2.3 AU had a 1–4% chance of striking the Earth. Test bodies from the 3:1 mean motion resonance with Jupiter (J3:1) at 2.5 AU had impact probabilities that were a factor of 5 lower than this value, while those resonances beyond the J3:1 were orders of magnitude lower. The location of many notable main belt resonances are shown in Fig. 11.

We infer from this that the H chondrites and HED meteorites were likely to be derived from asteroid families with the following characteristics: (1) they are capable of producing numerous meteoroids via collisional cascades, implying that they are young enough to have a steep FSD and/or large enough that even their steady-state meteoroid output is relatively high, and (2) they have access to efficient dynamical pathways for delivering material to Earth,

presumably resonant pathways with a <2.3 AU or via the powerful J3:1 resonance (Bottke et al. 2005a, 2005b, 2006a). Links between the Vesta family in the inner main belt and the HEDs have been established (e.g., Binzel and Xu 1993; Keil 2002). Plausible source families for the H chondrites will be discussed below.

Provenance of the Meteorites Containing CM Clasts

It seems unlikely that the current crop of CM clasts were present when the H5 Plainview and H6 Abbott portions of the H-chondrite parent body were metamorphosed or when the HED parent body was melted early in solar-system history. If the clasts had been present, all of them would have been heated and dehydrated (or, in the case of those on the HED body, melted). The extant CM clasts must instead have been introduced to the H and HED parent bodies after these bodies had cooled. Because these clasts were incorporated into regolith breccias, the main asteroid belt must have been undergoing sufficient collisional activity to produce regoliths on asteroid surfaces.

Without precise ages for the CM clasts and their host rocks, we can only speculate on the timing of delivery of CM clasts to the H and HED parent bodies. The flux of CM-like material estimated from lunar soils was high 3.9 Ga ago and has been fairly steady for the last 3.5 Ga. It is thus possible that the CM clasts were delivered ~3.9 Ga ago when the lunar CM flux was highest. However, the AB3-like CM clasts are not ubiquitous; they are relatively common in H and HED regolith breccias and are rare to absent in other meteorite types (e.g., Keil 1982). Presumably, all meteorite parent bodies and/or their fragments were exposed to this constant rain of debris at some level over the last 3.9 Ga.

The host H or HED regoliths that include unshocked or lightly shocked volatile-rich CM-clasts like AB3 or AB8 (hereafter AB3-like CM clasts) were produced either on the hosts' original parent bodies via spall from larger CM projectiles, with the regolith breccias produced on the parent body ejected at some later time by impacts, or on fragments derived from these bodies that were large enough to produce regoliths (e.g., multi-kilometer objects) via smaller CM projectiles. While both may have been relevant at some time and at some level, the dominant delivery mechanism likely favored the introduction of CM-chondrite material into H and HED regolith breccias. Below we present some different hypotheses to account for these constraints. (The complementary work of Gounelle et al. [2003] discusses the nature and delivery of CM clasts into HED meteorites).

Scenario 1. The CM Clasts Formed on Ancient Families

One way to account for the inference that H chondrite and HED families were more likely to have incorporated CM projectiles than other meteorite parent bodies/families is to assume that their source families are extremely old. This would allow them to have witnessed billions of years of CM-like micrometeorite impacts. If they were old enough, they might even have been around during the epoch 3.7–3.9 Ga ago when the Moon is believed to have experienced a high impact flux (i.e., this period is often referred to as the lunar Late Heavy Bombardment; e.g., Levison et al. 2001).

Asteroid families have advantages over single parent bodies in terms of target area for micrometeorites. The cross-sectional area of a spherical parent body is $\pi \cdot r^2$, where r is the radius of the parent body. The combined cross section area of an asteroid family, however, is the summation of $\pi \cdot r^2$ for every fragment capable of producing a regolith breccia. Testing this against the derived size-frequency distributions and parent body sizes of existing families (Durda et al. 2007), we find that the combined surface area of most families is 1–3 orders of magnitude larger than that of the original parent body. This means that, all things being equal, ancient families are likely to have experienced many more CM-like impacts from centimeter-size projectiles than individual parent bodies or young families.

Is there any evidence that the H and HED families are older than the source families for other meteorite groups? The parent body and parent family for the HEDs are commonly assumed to be 4 Vesta and the Vesta family (vestoids; see Fig. 11). While collisional and dynamical modeling work on the Vesta family yield ambiguities in age (e.g., Nesvorný et al. 2005, 2008), there are numerous ^{39}Ar-^{40}Ar shock-degassing events recorded in eucrites between 3.3 and 4.1 Ga (Bogard 1995, 2005). It is plausible that the Vesta-family-forming event (or events) marks one of these collisionally induced degassing episodes.

The Ar-Ar age signatures of the L chondrites show a very prominent peak at 470 Ma (Korochantseva et al. 2007) and a few events between 3.5–4.2 Ga (Bogard 1995). The oft-cited interpretation is that the L-chondrite parent body disrupted 470 Ma ago (e.g., Nesvorný et al. 2007, 2009), presumably making the L-chondrite source family ~3 Ga younger than the Vesta family. The Ar-Ar data on LL chondrites are limited and ambiguous, but the few events measured to date have ages near 1.2 Ga and 3.5–4.2 Ga (Bogard 1995). [Note that Nesvorný et al. (2009) make the case that the Gefion family is the source of the L chondrites (see Fig. 11)].

While the timing of the H-chondrite-family-forming event is unknown, the H chondrites were affected by numerous Ar-Ar shock-degassing events 3.4–4.1 Ga ago as well as within the last 600 Ma. Overall, the most prominent Ar-Ar features occurred within the last 250–325 Ma (Bogard 1995; Grier et al. 2004; Swindle et al. 2009). While we do not know if the 250–325 Ma and 3.4–4.1 Ga events produced any asteroid families, impact events energetic enough to produce Ar-Ar shock degassing events should also have produced a moderate amount of ejecta. It is apparent that the measured Ar-Ar ages of H chondrites do not violate the hypothesis that AB3-like CM projectiles were incorporated into the regoliths of old H-chondrite family members.

If at least a portion of the H-chondrite family is ancient, candidate source families with the right taxonomic type and dynamical age would include Maria (estimated age of 3 ± 1 Ga), Koronis (estimated age of 2.5 ± 1 Ga), and Eunomia (2.5 ± 0.5 Ga) (Nesvorný et al. 2005) (Fig. 11). Of the three, Maria and Eunomia are adjacent to the J3:1 resonance and thus have the best potential to deliver meteorites efficiently to Earth. It is estimated that H chondrites produce 34% of all meteorite falls (Burbine et al. 2002). The only other meteorite group close to this value is the (even more abundant) L-chondrite group, which constitutes 38% of all falls.

In this scenario, what is the likely source of the CM clasts? Carvano et al. (2003) showed that numerous asteroids with CM-like spectroscopic signatures are found in the outer main belt. Accordingly, it is plausible that collisional grinding among asteroids in the outer main belt produces numerous CM-like particles that evolve inward via non-gravitational forces (e.g., Poynting-Robertson drag; Yarkovsky effect; Burns et al. 1979). If the debris is centimeter-size or smaller, it can drift inward rapidly enough to jump resonance after resonance (e.g., Bottke et al. 2000) on its way across the main belt. In some cases, the fragments may evolve and become very similar to those of main-belt families. This would allow the CM projectiles to land at the ≤300 m s^{-1} speeds inferred from the unshocked, volatile-rich AB3 and AB8 clasts (Bottke et al. 1994). The remaining CM projectiles would have struck the H-chondrite parent-body families and Vesta/vestoids at somewhat higher relative velocities. This could explain the dehydrated, shocked and annealed PV3 CM clast from the Plainview H-chondrite regolith breccia as well as a clast in the LEW 87295 polymict eucrite that contains dehydrated phyllosilicates (Zolensky et al. 1996).

The remaining factor needed to satisfy the somewhat limited constraints on this hypothesis is a set of numerous ancient collisions among CM-like main belt asteroids 3.4–4.1 Ga. Interestingly, recent work may provide the means to characterize the events that took place in the asteroid belt at this time.

We consider it plausible that the peak in the flux of CM-like material on the Moon as well as meteorite Ar-Ar shock ages near 3.4–4.1 Ga are related to the so-called Late Heavy Bombardment of the Moon and terrestrial planets (Levison et al. 2001; Morbidelli et al. 2005; Gomes et al. 2005; Tsiganis et al. 2005; Warren 2005) as well as the last major dynamical excitation event in the main belt (Gomes et al. 2005; Strom et al. 2005; Bottke et al. 2007a). New ideas about the Late Heavy Bombardment can be found in the Nice model (Morbidelli et al. 2005; Gomes et al. 2005; Tsiganis et al. 2005), which is the most successful model to date for explaining the characteristics of the outer solar system.

In the Nice model, the giant planets are assumed to have formed in a compact configuration; all were located between 5 and 15 AU. They were surrounded by a 35-Earth-mass disk of cometary planetesimals stretching between 16 and 30 AU. Slow migration was induced in the planets by gravitational interactions with planetesimals leaking out of this disk. After ~600 Ma, Jupiter and Saturn crossed their mutual 1:2 mean motion resonance, triggering a global instability in the orbits of the planets that led to a violent reorganization of the outer solar system. Uranus and Neptune penetrated the trans-planetary disk, scattering its inhabitants throughout the solar system. The interaction between the ice giants and the planetesimals damped the orbits of these planets, leading them to evolve into their current orbits.

For the asteroid belt, several important ramifications of the Nice model were recently explored by Levison et al. (2009). These include: (i) Uranus and Neptune entered the primordial disk and scattered comets throughout the solar system, (ii) several mean-motion resonances experienced a temporary transition in character, going from stable to chaotic and then back to stable again, and (iii) the migration of Jupiter and Saturn produced resonances that swept across much of the inner solar system. This combination led to the capture of comets deep within the Trojan, Hilda, and outer main belt regions. The black dots in Fig. 11 show the orbital properties of the representative model comets embedded within the outer main belt region from Levison et al. (2009) These model comets represent a population that was, at one time, many times larger than the existing Trojan asteroid population.

Levison et al. (2009) also showed that additional comets were injected along the periphery of the main belt into orbits that were unstable over timescales of several hundred Ma. If the Nice model instability occurred ~3.9 Ga ago, the prolonged residence time of these stable/unstable comets and their likely impacts onto indigenous main-belt asteroids provide a natural explanation for the timing of the Ar-Ar shock degassing ages between 3.4–4.1 Ga for many meteorite classes. Moreover, many embedded comets were probably weak enough that impacts with both themselves and stronger indigenous main-belt asteroids would have caused frequent disruption events, which in turn would have produced large quantities of micrometeoroids. In fact, collisional evolution calculations in Levison et al. (2009) indicate that the embedded comets in the main belt may be the dominant source of the unmelted micrometeorites found in Antarctica, most of which are similar to CI, CM, or CR-like meteorites (e.g., Kurat et al. 1994; Walter et al. 1995; Yada et al. 1997).

A drawback to the acceptance of this scenario is that no consensus has been reached on the source of the H chondrites; we cannot demonstrate that some H chondrites come from an ancient family and, thus, we cannot test this model. Moreover, the largest concentration of Ar-Ar shock ages for the H chondrites is at 250–340 Ma; as far as we know, this may be the only family-forming event associated with the H chondrites.

Similarly, we do not know the age of the Vesta family; it is conceivable that it is much younger than the Ar-Ar shock ages of the eucrites. It is also possible that some of the properties of the AB3-like CM projectiles inferred above

are incorrect. For example, if the clasts were derived from large impacts (e.g., material spalled off the back of a massive CM projectile), our conclusions would be incorrect.

Nevertheless, if we assume the formation of the AB3-like CM clasts is linked to the predictions made by the Nice model, the following events probably took place: (i) Comets were embedded in the outer asteroid belt 3.9–4.0 Ga ago. (ii) Collisional grinding induced by this new population, both among the comets themselves and by impacts onto indigenous outer main-belt asteroids, created copious amounts of CM-like and other primitive micrometeoroids. This potentially provided a source for the AB3-like CM-clasts as well as the influx of CM- or CI-like material to the Moon. The actual source of the CM clast material could have been either asteroids (e.g., comets slamming into CM-like indigenous asteroids thereby creating fragments) or comets (e.g., some of the disrupted comets were themselves CM-like). (iii) These embedded comets also hit other asteroids and produced the Ar-Ar shock degassing ages observed in different meteorite classes between 3.4–4.1 Ga. (iv) This bombardment produced ancient families related to the H and HED meteorites, allowing the family members to be exposed to the large influx of CM-like material for billions of years.

An argument that the CM-clasts came from the disruption of indigenous asteroids rather than comets comes from the similarities found among different chondrite groups (including hydrous and anhydrous meteorites) in bulk chemical and O-isotopic composition and in textures. These data suggest that the CM clasts were derived from similar bodies and that these are likely to be asteroids (e.g., Wasson and Wetherill 1979). If so, comets bombarding the asteroid belt during the Late Heavy Bombardment probably produced the putative ancient HED and H-chondrite families and liberated CM material from their parent bodies, with the small, mobile fragments being swept up by the aforementioned family members.

Scenario 2. The CM Clasts Formed on the H and HED Parent Bodies

This scenario builds on many of the attributes described in Scenario 1, except that here the CM clasts would be produced by spall fragments from larger CM-like projectiles. The sources for the projectiles are the same as in Scenario 1; primitive asteroids and/or embedded comets from the outer main belt.

Scenario 2 has certain advantages over Scenario 1. For example, the H and HED parent bodies, being significantly larger than any of their putative family members, can sustain more energetic impacts and can retain more regolith. Over time, these objects are likely to build up a substantial regolith that can be readily lithified by impact-driven shock events. The formation of most meteorite breccias on larger parent bodies rather than smaller family members provides a straightforward way to explain why the fraction of brecciated meteorites increases with inferred parent body size (Scott et al. 2009). Moreover, the H and HED parent bodies may be better able to absorb shock-producing impact events than their smaller family members (i.e., dead men tell no tales); this could explain the wide range of shock degassing ages seen among the H chondrites and HEDs.

The drawback to Scenario 2 is that many meteorite classes lack CM clasts. To explain their absence, we must assume that the H and HED parent bodies were "special" in some manner relative to other meteorite parent bodies. There are several ways this could take place (e.g., particular meteorite parent bodies may have been out of range of most outer main belt projectiles, large impact events capable of delivering numerous clasts are stochastic by nature, there are important meteorite sampling biases that need to be considered, etc.). In this vein, we find it interesting that the H and HED meteorites both have hydrated CM clasts and numerous Ar-Ar shock degassing ages between 3.4–4.1 Ga relative to other meteorite groups. If Scenario 2 is correct, this seems unlikely to be a coincidence.

Scenario 3. CM Clasts Produced by a Recent Disruption Event

An alternative to Scenarios 1 and 2 is that the CM clasts could have come from more recent impact events. If the prominent Ar-Ar shock degassing event in H-chondrite meteorites at 250–340 Ma is identical to the H-chondrite family-forming event, and the small projectile-CM clast delivery mechanism is valid, this would necessitate a very recent source of CM-like material capable of striking H-chondrite and Vesta family members at extremely low velocities. This would in turn imply that the CM source had to have been located near components of the Vesta and H-chondrite families. It would also mean that there is no direct connection between the CM- or CI-like material on the Moon and the source of the AB3-like CM clasts.

Here we speculate about a possible recent source for the CM clasts. Numerical simulations by Bottke et al. (2007a) indicate that 160 ± 20 Ma ago, the parent body of the Baptistina asteroid family (BAF), estimated to be a ~170-km-diameter C-complex (i.e., C-type and X-type spectra) asteroid, catastrophically disrupted in the innermost region of the main asteroid belt (Fig. 11). (We assume that the parent asteroid was relatively uniform in composition.) The BAF is thought to be the largest and youngest C-complex family in the inner main belt; it consists of >3000 member asteroids. Its 160-Ma age makes it younger than the Flora-family-forming event (~470 Ma ago; Schmitz et al. 2003; Nesvorný et al. 2007) and almost certainly younger than the Vesta-family-forming event (see above). The available evidence does not yet allow us to conclude whether the BAF was composed of CM-like material, but circumstantial evidence renders this plausible.

The largest remnant of the BAF is 298 Baptistina, a ~40-km-size body located at 2.26 AU (Knežević and Milani 2003). The spectroscopic signature of Baptistina itself is difficult to interpret; it is not a traditional C-type asteroid. Some workers claim that it is an Xc-type asteroid (Mothé-Diniz et al. 2005), others that it is something else entirely (e.g., Reddy et al. 2008). At this point, it is not even clear if it is spectroscopically related to other BAF members; if not, it could be an interloper, a fragment from the projectile that produced the BAF, or a highly-altered fragment covered with shocked material. Nevertheless, Baptistina family members, according to color data from the Sloan Digital Sky Survey (SDSS), are solidly C-complex, with at least 300 members having C-complex colors (Parker et al. 2008). [The Baptistina family was independently identified using Sloan Digital Sky Survey (SDSS) color data by Parker et al. (2008) and named after the largest C-complex body within the Baptistina cluster that was contained in their SDSS database].

The BAF has many interesting properties. For instance, numerical modeling work suggests that a bombardment produced by the BAF-disruption event is responsible for the steep non-saturated population of fresh 0.2–0.6 km diameter craters on 951 Gaspra, a 19 × 12 × 11 km S-type asteroid located near the BAF (Bottke et al. 2007a). (The osculating elements for Baptistina are a = 2.2641 AU, e = 0.0953, and i = 6.283; those for Gaspra are a = 2.2098 AU, e = 0.1731, and i = 4.101). If this is true, then it is plausible that numerous small impactors from the BAF struck other inner-main-belt asteroids.

The BAF is also nearly bisected by the 7:2 mean motion resonance with Jupiter (abbreviated J7:2) and the 5:9 mean motion resonance with Mars (M5:9) located at a = 2.2545 AU (Bottke et al. 2007b). Bottke et al. (2007a) found that ~15–20% of Baptistina's multi-kilometer-size fragments were either directly injected into J7:2/M5:9 or drifted into it via Yarkovsky thermal forces. Once there, the eccentricities of these bodies were pumped up to achieve terrestrial-planet-crossing orbits within a few Ma to several tens of Ma (Morbidelli and Nesvorný 1999). This produced a ~100 Ma long surge in the terrestrial planets' impact flux that effectively doubled the number of kilometer-size impactors striking those bodies over the last 160 Ma.

These same computations showed that there is a >90% probability that a large fragment from the BAF produced the K/T impact on Earth. If this connection is reasonable, we can glean insights into the composition of BAF members by analyzing what we know of the K-T impactor. An analysis of a 65 Ma old fossil meteorite found in a north Pacific oceanic core sample showed it to be a highly altered carbonaceous chondrite (Kyte 1998; Shukolyukov and Lugmair 1998). This is consistent with the C-complex nature of the BAF. Trinquier et al. (2006) found that the closest match between trace Cr signatures found at different K-T ejecta layer sites and the known meteorites are those found in CM2 carbonaceous chondrites. Thus, BAF members may have CM2-like compositions.

Here we assume that the Baptistina family is a prominent source of CM meteorites. Supporting evidence for the 160 ± 20 Ma age of the Baptistina family might come from irradiated grains found in the CM regolith breccias of Murchison, Murray and Cold Bokkeveld (Hohenberg et al. 1990). If the current energetic particle complex of the solar system is representative of time-averaged conditions, the minimum galactic cosmic-ray regolith exposure time needed for the most heavily irradiated grains to accumulate their observed cosmogenic Ne is 145 Ma. This age is remarkably similar to the inferred age of the Baptistina family and would imply that CM regolith breccias are mostly derived from the surfaces of BAF family members.

An alternative possibility raised by Hohenberg et al. (1990) is that these data are minimum ages for grains that were exposed and buried (perhaps multiple times) on the surface of the CM parent body via impact gardening processes. If so, this would favor Scenarios 1 and 2 (particularly the latter), because gardening is more likely to occur on ancient large bodies than on younger smaller ones. On the other hand, we note that numerical simulations of the Baptistina family-forming event indicate that the parent body experienced a super-catastrophic disruption event, with ~99% of the total mass of the parent body placed into bodies smaller than 20 km. When this information is combined with the surface area and volume arguments described for Scenario 1 above, we find it plausible that the CM clasts found in the regolith breccias reaching us today are from numerous Baptistina family members.

To summarize, the BAF is a very large, relatively young C/X-complex asteroid family in the innermost region of the main belt. It is located near some of the most efficient dynamical pathways capable of sending asteroids to Earth (e.g., the J7:2/M5:9 mean motion resonances, the υ6 secular resonance). Given our understanding of the processes controlling meteorite delivery, it is plausible that the BAF is the source of the most abundant group of carbonaceous chondrites, i.e., the CM group (Bottke et al. 2007a). This proposed link is strengthened by the connection between the probable composition of the K/T impactor (CM2) and the likelihood that the BAF produced that impactor. It is weakened, however, by the spectroscopic signature of 298 Baptistina (Reddy et al. 2008). Until additional data relevant to this hypothesis are identified, this issue will remain unresolved.

If the BAF indeed had a CM2-type composition, then ejecta from the BAF may be the major contributor to the population of projectiles that produced the CM clasts on the H and HED parent bodies. The BAF resides near numerous non-BAF asteroids with a <2.3 AU that would almost certainly have been struck by the fragments from the Baptistina parent body when it disrupted. The Vesta family, which extends from

the υ6 secular resonance (at 2.15 AU for these bodies) to the 3:1 mean motion resonance with Jupiter at 2.5 AU, could have been a prominent target (Fig. 11). According to terrestrial impact probability statistics computed for bodies escaping the main belt (Bottke et al. 2006a; see above), roughly an order of magnitude more HEDs passed through the υ6 resonance than the 3:1 resonance. This means that the precursors of the HEDs with CM clasts were much more likely to have resided near the υ6 resonance at 2.15 AU than the 3:1 resonance at 2.5 AU. A steady state population of HED meteoroids coming out of the υ6 resonance would also provide a reasonable explanation for the observed fall times of the HEDs, which show less preference for afternoon falls than other meteorite classes (e.g., Wetherill 1987; Morbidelli and Gladman 1998).

Let us assume that this region is a possible source of the H-chondrite regolith breccia precursor bodies. This would mean that the H-chondrite parent family is located in the inner main belt near the Baptistina family. The only prominent S-type family near that location is Flora, a somewhat sprawling family that potentially contains more than one family.

There are several reasons why we have not yet identified the H-chondrite parent family. First, the inner main belt is crisscrossed by numerous tiny resonances capable of modifying the eccentricities and inclinations of the objects passing through them over fairly short timescales. Numerical simulations of the dynamical evolution of the Flora family show that D < 30 km bodies drifting in semimajor axis by Yarkovsky effects are driven through multiple resonances, allowing them to fill the inner main belt zone with family members within 200 Ma (Nesvorný et al. 2002). For this reason, it is hard to say whether an older H-chondrite family residing near the prominent Flora family would even be recognizable using the standard cluster detection techniques. Second, the differences among ordinary-chondrite spectra are relatively small. If family members have had their surfaces altered by space-weathering processes (Clark et al. 2002), it is possible the families cannot easily be distinguished from one another. We also lack spectra on most of these objects. Third, we have yet to identify many of the kilometer-size objects in this region. Taken together, these issues make family identification in the inner main belt region challenging. Hence, we consider it possible, though perhaps unlikely, that components of the unknown H-chondrite parent family could be located in the same region of space as Flora.

If a small fraction of all BAF fragments obtained nearly identical orbits to those of the H and HED meteorite precursors, they would have very high collision probabilities and very low impact velocities (e.g., Bottke et al. 1994). To test whether fragments from the BAF could be delivered at low velocity to our putative H-chondrite family, we used the code described in Bottke et al. (1994) to compute the collision probabilities and impact velocities of both BAF members and background main-belt asteroids striking representative objects in the Flora family (i.e., 8 Flora and 951 Gaspra). We will assume that these objects are a reasonable proxy for the unknown orbits of H-chondrite family members that, according to the arguments provided above, are likely to reside in or near the Flora family.

For our background population, we chose the set of 682 main-belt asteroids with D > 50 km; we assume that these bodies represent a complete set across the main belt. For our BAF objects, we chose the >3000 known asteroids in the BAF family (Bottke et al. 2007a).

Our results indicate that the mean intrinsic collision probability (defined as the probability that a member of the impacting population will hit a unit area of the target body in a unit of time) for BAF members striking 8 Flora and 951 Gaspra was 4 times greater than that of background main-belt asteroids; (10 versus 2.5) × 10^{-18} km^{-2} yr^{-1}, respectively. Among BAF impactors striking 8 Flora and 951 Gaspra, ~0.2% hit at velocities less than 300 m s^{-1}. Virtually none of the background main-belt asteroids in our sample collided at such low relative velocities. Because velocities ≤300 m s^{-1} can be considered sufficiently "low" to prevent the projectiles from becoming highly shocked or melted (e.g., Fig. 1 of Hartmann 1979; Fig. 1 of Bischoff et al. 2006), our scenario provides a plausible explanation for the presence of unshocked clasts in the H and HED meteorites.

A disadvantage to this scenario is that the H-chondrite parent body/family may not have any components with a <2.3 AU. It is also far from certain that a clear link can be established between Baptistina family members and CM meteorites, although there is some circumstantial evidence for this (Bottke et al. 2007a). The apparent prevalence of CM-like material in the inner solar system over the last 3.9 Ga makes it increasingly likely that many different bodies have provided CM material to asteroid parent bodies, asteroid families and the Moon. However, even if this checks out, this scenario does not explain why CM clasts are largely absent from Flora family members, which are believed to be the source of the L (Nesvorný et al. 2007) or LL (Vernazza et al. 2008) chondrites. The fraction of regolith breccias in both these meteorite groups is fairly low, but invoking selection effects to explain the dearth or absence of CM clasts in these breccias seems unsatisfactory.

CONCLUSIONS

CM-like carbonaceous chondrite clasts are the most abundant variety of foreign clasts in H-chondrite and HED breccias. The clasts are petrologically diverse: many contain abundant phyllosilicates and tochilinite-cronstedtite intergrowths. They are fragments of relatively unshocked CM projectiles that accreted at low relative velocities to the regoliths of their host parent bodies. A few CM clasts were shock heated and dehydrated during impact; they probably

accreted at somewhat higher relative velocities. These clasts were later annealed, presumably by being buried by target debris heated by the same events involving the impacts of the CM projectiles to the regolith.

Here we focus on three different formation scenarios (each of which has both positive and negative attributes) for unshocked, volatile-rich CM clasts. In Scenario 1, we assumed that the large sizes inferred for the H and HED parent bodies (200–500 km in diameter) prevented small volatile-rich CM-clast precursors from landing at low velocities (<300 m s^{-1}). Accordingly, the CM clasts came from centimeter-size precursors that had orbits extremely similar to those of H and HED family members; this allowed the CM materials to accrete without causing dehydration.

In Scenario 2, we assumed that the CM clasts were incorporated into ancient components of the H and HED parent bodies via spall fragments from larger CM projectiles. In both Scenario 1 and 2, the clasts were potentially derived from outer main belt objects, many of which have CM-like spectroscopic signatures. A potential source for a sudden jump in the quantity of this material may have been comets embedded in the outer main belt 3.9–4.0 Ga via the events described in the Nice model. If correct, this scenario links the CM clasts to the events surrounding the lunar Late Heavy Bombardment, the 3.4–4.1 Ga shock degassing ages found on numerous meteorite classes, and the large quantity of CM- or CI-like material found in lunar soils.

In Scenario 3, we assumed that the CM clasts were young. A possible source for them would be the disruption ~160 Ma ago of the ~170-km-diameter parent body of the Baptistina asteroid family (BAF). This family, which consists of >3000 asteroids, is named after its largest member, the ~40-km-diameter asteroid 298 Baptistina. If the BAF is the source of the K-T impactor, as claimed by Bottke et al. (2007), BAF members may have a CM2-type composition.

Acknowledgments–We thank the curators at the Institute of Meteoritics, University of New Mexico for the loan of the Abbott and Plainview thin sections. This work was supported in part by NASA Cosmochemistry Grant NNG06GF95G (A. E. Rubin). Research funds for W. F. Bottke were provided by NASA's Origins of Solar Systems Program (Grant NNG05GI28G), the Planetary Geology and Geophysics Program (Grant NNG05GI28G) and the Near Earth Object Observation Program (Grant NNG06GG06G). We thank J. T. Wasson for useful comments, M. J. Gaffey, T. H. Burbine and M. Gounelle for helpful reviews, and associate editors A. J. Brearley and T. D. Swindle for valuable comments.

Editorial Handling—Dr. Timothy Swindle

REFERENCES

Akai J. 1990. Thermal metamorphism in four Antarctic carbonaceous chondrites and its temperature scale estimated by T-T-T diagram (abstract). *NIPR Symposium on Antarctic Meteorites* 15:86–87.

Anders E. 1978. Most stony meteorites come from the asteroid belt. In *Asteroids: An exploration assessment*, edited by Morrison D. and Wells W. C. NASA CP 2053. U.S. Government Print Office.

Ashworth J. R. and Mallinson L. G. 1985. Transmission electron microscopy of L-group chondrites, 2. Experimentally annealed Kyushu. *Earth and Planetary Science Letters* 73:33–40.

Bauer J. F. 1979. Experimental shock metamorphism of mono- and polycrystalline olivine: A comparative study. Proceedings, 10th Lunar and Planetary Science Conference. pp. 2573–2596.

Binzel R. P. and Xu S. 1993. Chips off of asteroid 4 Vesta: Evidence for the parent body of basaltic achondrite meteorites. *Science* 260:186–191.

Bischoff A., Scott E. R. D., Metzler K., and Goodrich C. A. 2006. Nature and origin of meteoritic breccias. In: *Meteorites and the early solar system II*, edited by Lauretta D. S. and McSween H. Y. Tucson, Arizona: The University of Arizona Press. pp. 679–712.

Bland P. A., Artemieva N. A., Collins G. S., Bottke W. F., Bussey D. B. J., and Joy K. H. 2008. Asteroids on the Moon: Projectile survival during low velocity impact (abstract #2045). 39th Lunar and Planetary Science Conference. CD-ROM.

Bogard D. 1995. Impact ages of meteorites: A synthesis. *Meteoritics* 30:244–268.

Bottke W. F., Nolan M. C., Kolvoord R. A., and Greenberg R. 1994. Velocity distribution among colliding asteroids. *Icarus* 107:255–268.

Bottke W. F., Rubincam D. P., and Burns J. A. 2000. Dynamical evolution of main belt meteoroids: Numerical simulations incorporating planetary perturbations and Yarkovsky thermal forces. *Icarus* 145:301–331.

Bottke W. F., Vokrouhlicky D., Broz M., Nesvorný D., and Morbidelli A. 2001. Dynamical spreading of asteroid families by the Yarkovsky effect. *Science* 294:1693–1696.

Bottke W. F., Vokrouhlický D., Rubincam D.P., and Brož M. 2002a. The effect of Yarkovsky thermal forces on the dynamical evolution of asteroids and meteoroids. In: *Asteroids III,* edited by Bottke W. F., Cellino A., Paolicchi P., and R. P. Binzel. Tucson, Arizona: The University of Arizona Press. pp. 395–408.

Bottke W. F., Morbidelli A., Jedicke R., Petit J.-M., Levison H., Michel P., and Metcalfe T. S. 2002b. Debiased orbital and size distributions of the near-Earth objects. *Icarus* 156:399–433.

Bottke W. F., Durda D. D., Nesvorný D., Jedicke R., Morbidelli A., Vokrouhlicky D., and Levison H. 2005a. The fossilized size distribution of the main asteroid belt. *Icarus* 175:111–140.

Bottke W. F., Durda D. D., Nesvorný D., Jedicke R., Morbidelli A., Vokrouhlicky D., and Levison H. F. 2005b. Linking the collisional history of the main asteroid belt to its dynamical excitation and depletion. *Icarus* 179:63–94.

Bottke W. F., Durda D., Nesvorný D., Jedicke R., Morbidelli A., Vokrouhlický D., and Levison H. 2005c. The origin and evolution of stony meteorites. In *Dynamics of populations of planetary systems*, edited by Knezevic Z., and Milani A. IAU Colloquium 197. pp. 357–374.

Bottke W. F., Nesvorný D., Grimm R. E., Morbidelli A., and O'Brien D. P. 2006a. Iron meteorites as remnants of planetesimals formed in the terrestrial planet region. *Nature* 439:821–824.

Bottke W. F., Vokrouhlicky D., Rubincam D. P., and Nesvorný D. 2006b. The Yarkovsky and YORP Effects: Implications for asteroid dynamics. *Annual Review of Earth and Planetary Science* 34:157–191.

Bottke W. F., Vokrouhlický D., Chapman C. R., and Nesvorný D. 2007a. Gaspra's steep crater population was produced by a large recent breakup in the main asteroid belt (abstract #2165). 38th Lunar and Planetary Science Conference. CD-ROM.

Bottke W. F., Vokrouhlický D., and Nesvorný D. 2007b. An asteroid breakup 160 Myr ago as the probably source of the K/T impactor. *Nature* 449:48–53.

Boyd F. R. and England J. L. 1965. The rhombic enstatite-clinoenstatite inversion. *Annual Report of the Director, Geophysical Laboratory.* Washington, D. C.: Carnegie Institution of Washington, pp. 117–120.

Brearley A. J. 1993. Carbonaceous chondrite clasts in the Kapoeta howardite (abstract). 24th Lunar and Planetary Science Conference. pp. 183–184.

Britt D. T., Yeomans D., Housen K., and Consolmagno G. 2002. Asteroid density, porosity, and structure. In *Asteroids III*, edited by Bottke W. F., Cellino A., Paolicchi P., and Binzel R. P. Tucson, Arizona: The University of Arizona Press. pp. 485–500.

Buchanan P. C., Zolensky M. E., and Reid A. M. 1993. Carbonaceous chondrite clasts in the howardites Bholgati and EET 87513. *Meteoritics* 28:659–669.

Bunch T. E., Chang S., Frick U., Neil J., and Moreland G. 1979. Carbonaceous chondrites—1. Characterization and significance of carbonaceous chondrite (CM) xenoliths in the Jodzie howardite. *Geochimica et Cosmochimica Acta* 43:1727–1742.

Burbine T. H., McCoy T. J., Meibom A., Gladman B., and Keil K. 2002. Meteoritic parent bodies: Their number and identification. In *Asteroids III*, edited by Bottke W. F., Cellino A., Paolicchi P., and Binzel R. P. Tucson, Arizona: The University of Arizona Press. pp. 653–667.

Burns J. A., Lamy P. L., and Soter S. 1979. Radiation forces on small particles in the solar system. *Icarus* 40:1–48.

Carvano J. M., Mothe-Diniz T., and Lazzaro D. 2003. Search for relations among a sample of 460 asteroids with featureless spectra. *Icarus* 161:356–382.

Christophe Michel-Lévy M., and Bourot-Denise M. 1988. A new look at the Galim (a) and Galim (b) meteorites. *Mineralogical Magazine* 52:519–525.

Clark B. E., Hapke B., Pieters C., and Britt D. 2002. Asteroid space weathering and regolith evolution. In *Asteroids III*, edited by Bottke W. F., Cellino A., Paolicchi P., and Binzel R. P. Tucson, Arizona: The University of Arizona Press. pp. 585–599.

Clayton R. N. and Mayeda T. K. 1999. Oxygen isotope studies of carbonaceous chondrites. *Geochimica et Cosmochimica Acta* 63: 2089–2104.

Dixon E. T., Bogard D. D., Garrison D. H., and Rubin A. E. 2004. ^{39}Ar-^{40}Ar evidence for early impact events on the LL parent body. *Geochimica et Cosmochimica Acta* 68:3779–3790.

Durda D., Bottke W. F., Nesvorný D., Encke B., Merline W. J., Asphaug E., and Richardson D. C. 2007. Size-frequency distributions of fragments from SPH/N-body simulations of asteroid impacts: Comparison with observed asteroid families. *Icarus* 186:498–516.

Farinella P., Froeschle C., and Gonczi R. 1993. Meteorites from the asteroid 6 Hebe. *Celestial Mechanics and Dynamical Astronomy* 56:287–305.

Fodor R. V. and Keil K. 1975. Implications of poikilitic textures in LL-group chondrites. *Meteoritics* 10:325–339.

Fodor R. V. and Keil K. 1976. Carbonaceous and noncarbonaceous lithic fragments in the Plainview, Texas chondrite: Origin and history. *Geochimica et Cosmochimica Acta* 40:177–189.

Fodor R. V., Keil K., Wilkening L. L., Bogard D. D., and Gibson E. K. 1976. Origin and history of a meteorite parent-body regolith breccia: Carbonaceous lithic fragments in the Abbott, New Mexico, chondrite. *Special Publications of the New Mexico Geological Society* 6:206–218.

Fuchs L. H., Olsen E., and Jensen K. J. 1973. Mineralogy, mineral-chemistry, and composition of the Murchison (C2) meteorite. *Smithsonian Contributions to the Earth Sciences* 10:1–39.

Gaffey M. J. and Gilbert S. L. 1998. Asteroid 6 Hebe: The probable parent body of the H-type ordinary chondrites and the IIE iron meteorites. *Meteoritics & Planetary Science* 33:1281–1295.

Gladman B. J., Migliorini F., Morbidelli A., Zappala V., Michel P., Cellino A., Froeschle C., Levison H. F., Bailey M., and Duncan M. 1997. Dynamical lifetimes of objects injected into asteroid belt resonances. *Science* 277:197–201.

Gomes R., Levison H. F., Tsiganis K., and Morbidelli A. 2005. Origin of the cataclysmic Late Heavy Bombardment period of the terrestrial planets. *Nature* 435:466–469.

Gounelle M., Zolensky M. E., Liou J.-C., Bland P. A., and Alard O. 2003. Mineralogy of carbonaceous chondritic microclasts in howardites: Identification of C2 fossil micrometeorites. *Geochimica et Cosmochimica Acta* 67:507–527.

Graf T. and Marti K. 1995. Collisional history of H chondrites. *Journal of Geophysical Research* 100:21247–21263.

Grady M. M. 2000. *Catalogue of meteorites*, 5th ed. Cambridge University Press. 689 p.

Greenwood R. C., Lee M. R., Hutchison R., and Barber D. J. 1994. Formation and alteration of CAIs in Cold Bokkeveld (CM2). *Geochimica et Cosmochimica Acta* 58:1913–1935.

Grier J. A., Kring D. A., Swindle T. D., Rivkin A. S., Cohen B. A., and Britt D. T. 2004. Analyses of the chondritic meteorite Orvinio (H6): Insight into the origins and evolution of shocked H chondrite material. *Meteoritics & Planetary Science* 39:1475–1493.

Grover J. E. 1972. The stability of low-clinoenstatite in the system $Mg_2Si_2O_6$-$CaMgSi_2O_6$ (abstract). *Transactions of the American Geophysical Union* 53:539.

Haggerty S. E. 1972. An enstatite chondrite from Hadley Rille (abstract). In *The Apollo 15 lunar samples*, edited by Chamberlain J. W. and Watkins C. pp. 85–87. Houston: Lunar and Planetary Institute.

Hartmann W. K. 1979. Diverse puzzling asteroids and a possible unified explanation. In: *Asteroids*, edited by Gehrels T. Tucson, Arizona: The University of Arizona Press. pp. 466–479.

Haskin L. A. and Warren P. H. 1991 Lunar chemistry. In: *Lunar sourcebook,* edited by Heiken G., Vaniman D., and French B. M. Cambridge University Press. pp. 357–474.

Hohenberg C. M., Nichols R. H., Jr., Olinger C. T., and Goswami J. N. 1990. Cosmogenic neon from individual grains of CM meteorites—Extremely long pre-compaction exposure histories or an enhanced early particle flux. *Geochimica et Cosmochimica Acta* 54:2133–2140.

Jarosewich E. 1990. Chemical analyses of meteorites: A compilation of stony and iron meteorite analyses. *Meteoritics* 25:323–337.

Jedicke R., Larsen J., and Spahr T. 2002. Observational selection effects in asteroid surveys. In *Asteroids III*, edited by Bottke W. F., Cellino A., Paolicchi P., and Binzel R. P. Tucson, Arizona: The University of Arizona Press. pp. 71–87.

Keil K. 1982. Composition and origin of chondritic breccias. In *Workshop on lunar breccias and soils and their meteoritic analogs*, edited by Taylor G. J. and Wilkening L. L. pp. 65–83, LPI Tech. Rpt. 82-02. Lunar and Planetary Institute, Houston.

Keil K. 2002. Geological history of asteroid 4 Vesta: The "smallest terrestrial planet." In *Asteroids III*, edited by Bottke W. F., Cellino A., Paolicchi P., and Binzel R. P. Tucson, Arizona: The University of Arizona Press. pp. 573–584.

Keil K. and Fodor R. V. 1980. Origin and history of the polymict-brecciated Tysnes Island chondrite and its carbonaceous and non-carbonaceous lithic fragments. *Chemie der Erde* 39:1–26.

Keil K., Fodor R. V., Starzyk P. M., Schmitt R. A., Bogard D. D., and Husain L. 1980. A 3.6-b.y.-old impact-melt rock fragment in the

Plainview chondrite: Implications for the age of the H-group chondrite parent body regolith formation. *Earth and Planetary Science Letters* 51:235–247.

Knežević Z. and Milani A. 2003. Proper element catalogs and asteroid families. *Astronomy and Astrophysics* 403:1165–1173.

Korochantseva E. V., Trieloff M., Lorenz C. A., Buykin A. I., Ivanova M. A., Schwarz W. H., Hopp J., and Jessberger E. K. 2007. L-chondrite asteroid breakup tied to Ordovician meteorite shower by multiple isochron ^{40}Ar-^{39}Ar dating. *Meteoritics & Planetary Science* 42:113–130.

Kozul J. and Hewins R. H. 1988. LEW 85300,02,03 polymict eucrites consortium—II: Breccia clasts, CM inclusion, glassy matrix and assembly history (abstract). 19th Lunar and Planetary Science Conference. pp. 647–648.

Kracher A., Keil K., Kallemeyn G. W., Wasson J. T., Clayton R. N., and Huss G. I. 1985. The Leoville (CV3) accretionary breccia. Proceedings, 16th Lunar and Planetary Science Conference. pp. D123–D135.

Kurat G., Koeberl C., Presper T., Brandstätter F., and Maurette M. 1994. Petrology and geochemistry of Antarctic micrometeorites. *Geochimica et Cosmochimica Acta* 58:3879–3904.

Kyte F. T. 1998. A meteorite from the Cretaceous-Tertiary boundary. *Nature* 396:237–239.

Levison H. F., Dones L., and Duncan M. J. 2001. The origin of Halley-type comets: Probing the inner Oort cloud. *Astronomical Journal* 121:2253–2267.

Levison H. F., Bottke W. F., Gounelle M., Morbidelli A., Nesvorný D., and Tsiganis K. 2009. Embedding comets in the asteroid belt. *Nature* 459.

Lipschutz M. E., Gaffey M. J., and Pellas P. 1989. Meteoritic parent bodies: Nature, number, size and relation to present-day asteroids. In *Asteroids III*, edited by Bottke W. F., Cellino A., Paolicchi P., and Binzel R. P. Tucson, Arizona: The University of Arizona Press. pp. 740–777.

MacPherson G. J. and Davis A. M. 1994. Refractory inclusions in the prototypical CM chondrite, Mighei. *Geochimica et Cosmochimica Acta* 58:5599–5625.

MacPherson G. J., Jarosewich E., and Lowenstein P. 1993. Magombedze: A new H-chondrite with light-dark structure. *Meteoritics* 28:138–142.

McSween H. Y. 1976. A new type of chondritic meteorite found in lunar soil. *Earth and Planetary Science Letters* 31:193–199.

Melosh H. J. 1989. *Impact cratering: A geologic process*. Oxford University Press, New York, 245 pp.

Metzler K., Bischoff A., and Stöffler D. 1992. Accretionary dust mantles in CM chondrites: Evidence for solar nebula processes. *Geochimica et Cosmochimica Acta* 56:2873–2897.

Migliorini F., Manara A., Scaltriti F., Farinella P., Cellino A., and di Martino M. 1997. Surface properties of (6) Hebe: A possible parent body of ordinary chondrites. *Icarus* 128:104–113.

Morbidelli A. and Gladman B. 1998. Orbital and temporal distributions of meteorites originating in the asteroid belt. *Meteoritics & Planetary Science* 33:999–1016.

Morbidelli A. and Nesvorný D. 1999. Numerous weak resonances drive asteroids toward terrestrial planet orbits. *Icarus* 139:295–308.

Morbidelli A., Levison H. F., Tsiganis K., and Gomes R. 2005. Chaotic capture of Jupiter's Trojan asteroids in the early solar system. *Nature* 435:462–465.

Mothé-Diniz T., Roig F., and Carvano J. M. 2005. Reanalysis of asteroid families structure through visible spectroscopy. *Icarus* 174:54–80.

Nesvorný D., Ferraz-Mello S., Holman M., and Morbidelli A. 2002. Regular and chaotic dynamics in the mean-motion resonances: Implications for the structure and evolution of the asteroid belt. In *Asteroids III*, edited by Bottke W. F., Cellino A., Paolicchi P., and Binzel R. P. Tucson, Arizona: The University of Arizona Press. pp. 379–394.

Nesvorný D., Bottke W. F., Levison H. F., and Dones L. 2003. Recent origin of the solar system dust bands. *The Astrophysical Journal* 591:486–497.

Nesvorný D., Jedicke R., Whiteley R. J., and Ivezic Z. 2005. Evidence for asteroid space weathering from the Sloan Digital Sky Survey. *Icarus* 173:132–152.

Nesvorný D., Vokrouhlický D., Bottke W. F., Gladman B., and Haggstrom T. 2007. Express delivery of fossil meteorites from the inner asteroid belt to Sweden. *Icarus* 188:400–413.

Nesvorný D., Vokrouhlický D., Morbidelli A., Bottke W. F. 2009. Asteroidal source of L chondrite meteorites. *Icarus* 200:698–701.

Nozette S. and Wilkening, L. L. 1982. Evidence for aqueous alteration in a carbonaceous xenolith from the Plainview (H5) chondrite. *Geochimica et Cosmochimica Acta* 46:557–563.

Parker A. H., Ivezić Z., Jurić M., Lupton R. H., Sekora M. D., and Kowalski A. F. 2008. The size distributions of asteroid families in the SDSS Moving Object Catalog 4. *Icarus* 198:138–155.

Peterson C. 1976. A source mechanism for meteorites controlled by the Yarkovsky effect. *Icarus* 29:91–111.

Pun A. 1992. Kapoeta: Implications for the igneous history and regolith evolution of the HED parent body. M.S. Thesis, Univ. New Mexico, 171 pp.

Reddy V., Kelley M. S., Emery J. P., Gaffey M. J., Bottke W. F., Nesvorný D., Schaal M., Cramer A., and Takir D. 2008. Composition of 298 Baptistina: Implications for K-T impactor link. *Asteroids, Comets, Meteors 2008*, abstract# 8243.

Rubin A. E. 1982. Petrology and origin of brecciated chondritic meteorites. Ph.D. thesis, University of New Mexico, Albuquerque, New Mexico.

Rubin A. E. 1992. A shock-metamorphic model for silicate darkening and compositionally variable plagioclase in CK and ordinary chondrites. *Geochimica et Cosmochimica Acta* 56:1705–1714.

Rubin A. E. 1997a. The Galim LL/EH polymict breccia: Evidence for impact-induced exchange between reduced and oxidized meteoritic material. *Meteoritics & Planetary Science* 32:489–492.

Rubin A. E. 1997b. The Hadley Rille enstatite chondrite and its agglutinate-like rim: Impact melting during accretion to the Moon. *Meteoritics & Planetary Science* 32:135–141.

Rubin A. E. 2000. Petrologic, geochemical and experimental constraints on models of chondrule formation. *Earth Science Reviews* 50:3–27.

Rubin A. E. 2004. Post-shock annealing and post-annealing shock in equilibrated ordinary chondrites: Implications for the thermal and shock histories of chondritic asteroids. *Geochimica et Cosmochimica Acta* 68:673–689.

Rubin A. E. 2006. Shock, post-shock annealing, and post-annealing shock in ureilites. *Meteoritics & Planetary Science* 41:125–133.

Rubin A. E. 2007. Petrography of refractory inclusions in CM2.6 QUE 97990 and the origin of melilite-free spinel inclusions in CM chondrites. *Meteoritics & Planetary Science* 42:1711–1726.

Rubin A. E. and Wasson J. T. 1986. Chondrules in the Murray CM2 meteorite and compositional differences between CM-CO and ordinary chondrite chondrules. *Geochimica et Cosmochimica Acta* 50:307–315.

Rubin A. E., Keil K., Taylor G. J., Ma M.-S., Schmitt R. A., and Bogard D. D. 1981. Derivation of a heterogeneous lithic fragment in the Bovedy L-group chondrite from impact-melted porphyritic chondrules. *Geochimica et Cosmochimica Acta* 45: 2213–2228.

Rubin A. E., Scott E. R. D., Taylor G. J., Keil K., Allen J. S. B., Mayeda T. K., Clayton R. N., and Bogard D. D. 1983. Nature of

the H chondrite parent body regolith: Evidence from the Dimmitt breccia. Proceedings, 13th Lunar and Planetary Science Conference. pp. A741–A754.

Rubin A. E., Scott E. R. D., and Keil K. 1997. Shock metamorphism of enstatite chondrites. *Geochimica et Cosmochimica Acta* 61: 847–858.

Rubin A. E., Ulff-Møller F., Wasson J. T., and Carlson W. D. 2001. The Portales Valley meteorite breccia: Evidence for impact-induced metamorphism of an ordinary chondrite. *Geochimica et Cosmochimica Acta* 65:323–342.

Rubin A. E., Trigo-Rodriguez J. M., Kunihiro T., Kallemeyn G. W., and Wasson J. T. 2005. Carbon-rich chondritic clast PV1 from the Plainview H-chondrite regolith breccia: Formation from H3 chondrite material by possible cometary impact. *Geochimica et Cosmochimica Acta* 69:3419–3430.

Rubin A. E., Trigo-Rodríguez J. M., Huber H., and Wasson J. T. 2007. Progressive aqueous alteration of CM carbonaceous chondrites. *Geochimica et Cosmochimica Acta* 71:2361–2382.

Schmitz B., Haggstrom T., and Tassinari M. 2003. Sediment-dispersed extraterrestrial chromite traces a major asteroid disruption event. *Science* 300:961–964.

Shukolyukov A. and Lugmair G. W. 1998. Isotopic evidence for the Cretaceous-Tertiary impactor and its type. *Science* 282:927–930.

Schultz L. and Kruse H. 1989. Helium, neon, and argon in meteorites—A data compilation. *Meteoritics* 24:155–172.

Scott E. R. D., Taylor G. J., Rubin A. E., Okada A., and Keil K. 1981a. Graphite-magnetite aggregates in ordinary chondritic meteorites. *Nature* 291:544–546.

Scott E. R. D., Rubin A. E., Taylor G. J., and Keil K. 1981b. New kind of type 3 chondrite with a graphite-magnetite matrix. *Earth and Planetary Science Letters* 56:19–31.

Scott E. R. D., Bogard D. D., Bottke W. F., Taylor G. J., Greenwood R. C., Franchi I. A., Keil K., Moskovitz N. A., and Nesvorný D. 2009. Impact histories of Vesta and vestoids inferred from howardites, eucrites, and diogenites. 40th Lunar and Planetary Science Conference. Abstract #2295.

Simon S. B., Grossman L., Hutcheon I. D., Phinney D. L., Weber P. K., and Fallon S. J. 2006. Formation of spinel-, hibonite-rich inclusions found in CM2 carbonaceous chondrites. *American Mineralogist* 91:1675–1687.

Stöffler D., Keil K., and Scott E. R. D. 1991. Shock metamorphism of ordinary chondrites. *Geochimica et Cosmochimica Acta* 55: 3845–3867.

Strom R. G., Malhotra R., Ito T., Yoshida F., and Kring D. A. 2005. The origin of planetary impactors in the inner solar system. *Science* 309:1847–1850.

Swindle T. D., Isachsen C. E., Weirich J. R., and Kring D. A. 2009. ^{40}Ar-^{39}Ar ages of H-chondrite impact melt breccias. *Meteoritics & Planetary Science.* This issue.

Tomeoka K. and Buseck P. R. 1985. Indicators of aqueous alteration in CM carbonaceous chondrites: microtextures of a layered mineral containing Fe, S, O and Ni. *Geochimica et Cosmochimica Acta* 49:2149–2163.

Tomeoka K., Kojima H., and Yanai K. 1989. Yamato-86720: A CM carbonaceous chondrite having experienced extensive aqueous alteration and thermal metamorphism. *Proceedings of the NIPR Symposium on Antarctic Meteorites* 2:55–74.

Trigo-Rodríguez J. M., Rubin A. E., and Wasson J. T. 2006. Non-nebular origin of dark mantles around chondrules and inclusions in CM chondrites. *Geochimica et Cosmochimica Acta* 70:1271–1290.

Trinquier A., Birck J.-L., and Allègre J. C. 2006. The nature of the K/T impactor. A ^{54}Cr reappraisal. *Earth and Planetary Science Letters* 241:780–788.

Tsiganis K., Gomes R., Morbidelli A., and Levison H. F. 2005. Origin of the orbital architecture of the giant planets of the solar system. *Nature* 435:459–461.

Vernazza P., Binzel R. P., Thomas C. A., Demeo F. E., Bus S. J., Rivkin A. S., and Tokunaga A. T. 2008. Compositional differences between meteorites and near-Earth asteroids. *Nature* 454:858–860.

Walter J., Kurat G., Brandstätter F., Koeberl C., and Maurette M. 1995. The abundance of ordinary chondrite debris among Antarctic micrometeorites. *Meteoritics* 30:592–593.

Warren P. H. 2005. The Moon. In: *Meteorites, comets and planets*, edited by Davis A. M. Treatise on Geochemistry, vol. 1. Elsevier, Amsterdam. pp. 559–599.

Wasson J. T. and Wetherill G. W. 1979. Dynamical, chemical and isotopic evidence regarding the formation locations of asteroids and meteorites. In *Asteroids*, edited by Gehrels T. Tucson, Arizona: The University of Arizona Press. pp. 926–974.

Wasson J. T., Boynton W. V., Chou C.-L., and Baedecker P. A. 1975. Compositional evidence regarding the influx of interplanetary materials onto the lunar surface. *Moon* 13:121–141.

Wetherill G. W. 1987. Dynamical relations between asteroids, meteorites and Apollo-Amor objects. *Royal Society of London Philosophical Transactions Series* 323:323–337.

Wilkening L. L. 1973. Foreign inclusions in stony meteorites—I. Carbonaceous xenoliths in the Kapoeta howardite. *Geochimica et Cosmochimica Acta* 37:1985–1989.

Wilkening L. L. 1976. Carbonaceous chondritic xenoliths and planetary-type noble gases in gas-rich meteorites. Proceedings, 7th Lunar Science Conference. pp. 3549–3559.

Wilkening L. and Clayton R. N. 1974. Foreign inclusions in stony meteorites—II. Rare gases and oxygen isotopes in a carbonaceous chondritic xenolith in the Plainview gas-rich chondrite. *Geochimica et Cosmochimica Acta* 38:937–945.

Wilshire H. G., Stuart-Alexander D. E., and Schwarzman E. D. 1997. Petrology and distribution of returned samples, Apollo 16. webpage: www.hq.nasa.gov/office/pao/History/alsj/a16/E-Petrology-Distribution.pdf.

Yada T., Yano H., Nakamura T., and Takaoka N. 1997. Comparisons of unmelted Antarctic micrometeorites with CM chondrites in petrology and mineralogy. *Meteoritics & Planetary Science* 32: A144.

Zolensky M. E. 1984. Hydrothermal alteration of CM carbonaceous chondrites; implications of the identification of tochilinite as one type of meteoritic PCP (abstract). *Meteoritics* 19:346–347.

Zolensky M. E. 1997. Structural water in the Bench Crater chondrite returned from the Moon. *Meteoritics* 32:15–18.

Zolensky M. E., Hewins R. H., Mittlefehldt D. W., Lindstrom M. M., Xiao X., and Lipschutz M. E. 1992. Mineralogy, petrology and geochemistry of carbonaceous chondritic clasts in the LEW 85300 polymict eucrite. *Meteoritics* 27:596–604.

Zolensky M. E., Weisberg M. K., Buchanan P. C., and Mittlefehldt D. W. 1996. Mineralogy of carbonaceous chondrite clasts in HED achondrites and the Moon. *Meteoritics & Planetary Science* 31:518–537.

Zook H. A. 1975. The state of meteoritic material on the Moon. Proceedings, 6th Lunar Science Conference. pp. 1653–1672.